Bioprinting 44 (2024) e00376

Contents lists available at ScienceDirect

Bioprinting

journal homepage: www.sciencedirect.com/journal/bioprinting

Advancements in high-resolution 3D bioprinting: Exploring technological trends, bioinks and achieved resolutions

Luca Guida *, Marco Cavallaro, Marinella Levi

Department of Chemistry, Materials and Chemical Engineering "Giulio Natta", Politecnico di Milano, Piazza Leonardo da Vinci 32, 20133, Milano, Italy

ARTICLE INFO

Keywords:
3D bioprinting
Resolution
Tissue engineering
Bioink
Characterization

ABSTRACT

3D bioprinting is a rapidly evolving field that has seen significant advancements in technologies, materials, and strategies. It enables the production of living tissues and complex biological structures, offering great potential for regenerative medicine, drug testing, and personalized medical treatments.

Notable progress has been done, particularly in developing materials that mimic the physiological environment and promote tissue growth. However, much work is still needed to fabricate complex, large-scale, heterocellular constructs. High-resolution printing and technological development are crucial to this goal.

Despite the significance of this topic, the literature lacks comprehensive reviews focused on analyzing the achieved resolution and metrics for its quantification in bioprinting. Additionally, no previous work examines all the most relevant technologies, critically highlighting technological advantages such as resolution and identifying limitations like the characteristic dimensions of constructs.

This review examines various aspects of 3D bioprinting, focusing on the most commonly used technologies, including Extrusion-Based Bioprinting, Vat Photopolymerization, Inkjet, Laser-Induced Forward Transfer, and Two-Photon Polymerization. Additionally, it examines the biomaterials and crosslinking strategies compatible with each of these technologies.

The primary focus is on the importance of resolution characterization, assessing technical advantages, and summarizing common metrics from the literature. The review evaluates the resolutions achieved across different bioprinting methods, correlating such data with the applicability and limitations of each technology, as resolution alone is not sufficient for producing functional structures. Some strategies to overcome typical resolution limits of some technologies have been reported.

In doing so, the focus is kept on works aimed at biological patterning and producing scaffolds for tissue engineering, therefore involving the use of live cells.

1. Introduction

3D bioprinting (3DB) is defined as the fabrication, through additive manufacturing techniques, of three-dimensional functional living constructs. Such technology involves the precise layer-wise deposition of biological materials and living cells (together termed bioink) into spatially defined structures through the use of automated machines (3D bioprinters) [1].

3DB has proven various advantages if compared with traditional biofabrication techniques, including higher precision and geometrical complexity, enhanced resolution and control in cell deposition, feasibility of co-culturing cells in a spatial organization [2].

The utilization of 3DB in scaffold construction allowed the production of advanced microstructures and precise anatomical features, together with the mimicry of the physiology of native tissues and even the pathological characteristics of diseases [2].

* Corresponding author.
E-mail address: luca.guida@polimi.it (L. Guida).

https://doi.org/10.1016/j.bprint.2024.e00376
Received 8 August 2024; Received in revised form 24 October 2024; Accepted 27 November 2024
Available online 28 November 2024
2405-8866/© 2024 The Authors. Published by Elsevier B.V. This is an open access article under the CC BY license (http://creativecommons.org/licenses/by/4.0/).

Thanks to the enhanced complexity achievable, 3DB has found several applications in regenerative medicine, though the fabrication of scaffolds mimicking natural tissues, and drug discovery research, allowing the production of complex in-vitro models and organs-on-a-chip [2,3].

The fabrication process relies on the deposition of bioinks containing living cells, which have been defined as "a formulation of cells suitable for processing by an automated biofabrication technology that may also contain biologically active components and biomaterials" [4]. Such comprehensive definition takes into account that different bioink properties are essential depending on the approach and technology exploited.

In scaffold-based 3DB, cells are loaded in an exogenous material, typically a hydrogel based on natural or synthetic polymers, which sustains the structure and favors cell spreading, growth, and differentiation. In scaffold-free 3DB, cells are deposited within aqueous media without the use of exogenous biomaterials, preferring self-assembly and mimicking embryonic development [3].

1.1. 3D bioprinting technologies

To date, various different additive manufacturing technologies are adopted for 3DB, each of them showing specific advantages, although no single bioprinting technique enables the production of all scales and complexities of natural tissues [5]. Major bioprinting techniques include Extrusion-Based Bioprinting (EBB) [6,7], inkjet [8], Laser Induced Forward Transfer (LIFT) [9], Vat Photopolymerization (VP) [10], and Two-Photon Polymerization (2PP) [11] (Fig. 1).

1.1.1. Extrusion-based bioprinting

In EBB, a bioink is loaded into a syringe barrel and is extruded through a micro-nozzle tip onto a build plate. Extrusion can be pneumatic, through the application of a hydrostatic pressure on the material, or mechanical (piston- or screw-driven).

An extrusion-based bioprinter may accommodate multiple print heads allowing multi-material 3DB [12].

Compared to inkjet-based and laser-based bioprinting, it can print higher cell densities and more viscous bioinks [13,14]. The easy setup required and the huge freedom in material selection have made EBB the most used technology in the field. However, the resolution of this technology is typically lower when compared with other ones and extrusion-related shear stresses during the flow in the nozzle can lead to cell damage/death [12].

1.1.2. Inkjet bioprinting

Inkjet printers use printheads that eject single drops of ink, contained in a reservoir. Depending on actuation type, thermal and piezoelectric inkjet printers are defined [15].

In thermal inkjet printing, an electrode is present next to the nozzle, able to locally heat the ink and form of a vapour bubble, which expands until explosion, ejecting a drop of ink.

In piezoelectric inkjet printing, a piezoelectric actuator is placed at the reservoir wall, able to cause a sudden deformation of the chamber wall and the expulsion of a drop [15].

Inkjet printing offers the advantage of contactless printing, limiting cross-contamination issues, and allows the generation of very small droplets (with a volume as small as tens of picoliters) [16].

On the other hand, limited ink viscosity is needed for this technology, with consequences both on the mechanical properties of final constructs

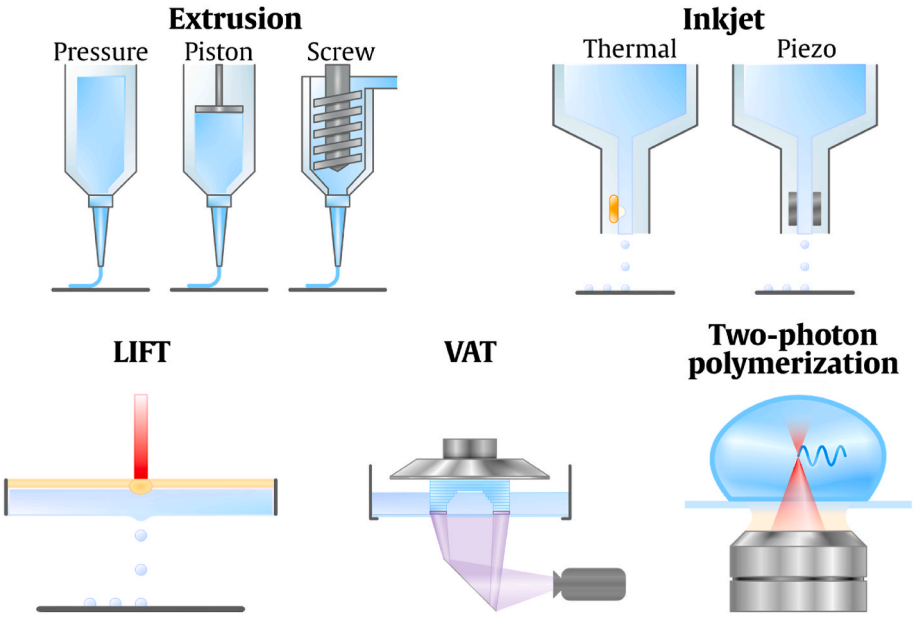

Fig. 1. Schematic representation of 3D bioprinting technologies. Figure redrawn from ref. [15,22].

and on cell sedimentation during printing with subsequent nozzle clogging [17–19]. Furthermore, the limited nozzle diameter leads to cells being subjected to shear stress during expulsion [16].

1.1.3. Laser induced forward transfer

LIFT is based on the transfer of a bioink from a donor ribbon onto a substrate through the use of a laser beam [15]. A typical apparatus comprises a laser source, a donor ribbon and a collector substrate. The donor ribbon corresponds to a transparent glass substrate coated with an energy-absorbing layer and a bioink layer.

Upon laser irradiation, the absorbing layer undergoes rapid heating, leading to vaporization and formation of a vapour bubble. The bubble's expansion generates a propulsive force, expelling a droplet of bioink which is deposited onto the collector substrate [15].

Compared with inkjet and extrusion printing methods, LIFT grants high printing resolution (up to the micron level), high throughput, and high cell survival rate [20]. In addition, being a non-contact technology, the risk of cross-contamination is minimized. Thanks to the absence of nozzles, shear-stress induced cellular damage and clogging-related issues are avoided. The high cost of LIFT technology is a significant factor limiting its research and commercial application [21].

1.1.4. Vat photo-polymerization

VP is a family of technologies using UV and visible light to selectively crosslink a photopolymer resin in a layer-wise manner. The photopolymer is initially contained into a vat, and it adheres onto a moving building plate upon solidification [22].

Three distinct light patterning techniques have been developed: Stereolithography (SLA) printing employs a laser spot to scan precise patterns, Liquid Crystal Display (LCD) printing utilizes an LCD screen to selectively irradiate specific areas of the bioink, while Digital Light Processing (DLP) printing employs a digital micromirror to project UV light patterns [23].

Once a layer has been completed, the build stage is moved into the photopolymer vat and the next layer is built directly on top of the previous layer [24].

Low-viscosity bioinks (0.25 to 10 Pa s) are preferred for VP as they improve curing rate and print accuracy, while decreasing construction time. Instead, low-viscosity leads to undesirable cell sedimentation during printing resulting in poor cell homogeneity within the bioprinted constructs [25].

VP mostly operates with a mono-material approach, despite the presence in literature of some works integrating multiple materials. However, these attempts often face challenges in achieving full automation due to inherent complexities in material handling and cross-contamination issues [26].

1.1.5. Two-Photon Polymerization

2PP is a laser-based photo-crosslinking technology able to bioprint three-dimensional micro- and nano-structures [27,28].

Using a high numerical aperture objective, a femtosecond laser beam can be focused into a very limited region of photocurable bioink. Due to the high density of photons within each pulse, two-photon absorption can take place and trigger the crosslinking of monomers within the focal volume. The characteristic energy of a photon (usually 780 nm) in 2PP is much lower than that of the traditional UV/Vis ones, which can greatly reduce damages to cells [29].

Resolution smaller than 100 nm is possible, enabling the investigation of constructs on a completely new scale [30].

It is important to notice that the typical dimension of parts fabricated via 2PP is significantly smaller than 1 mm, therefore the technology is not convenient for the production of or macroscopic structures (i.e. scaffolds for implantation). The fabricated structures are, however, precious in the investigation of cell-scaffold interactions [31].

1.2. Objectives of this review

Over the past decade, the field of 3DB has witnessed an exponential surge in scientific literature, comprising several studies dedicated to advancing novel materials and fabricating intricate structures tailored for diverse applications. This surge in literature has also been accompanied by numerous comprehensive reviews that summarize the current state-of-the-art in various aspects of the field. Indeed, numerous reviews have been dedicated to consolidating recent advancements in the utilization of specific bioink materials, such as GelMA, alginate, collagen, or synthetic polymers. Similarly, other reviews have focused on detailing progress in fabricating particular tissues or organs.

Additional reviews focus on individual materials used for specific tissue types or exploiting certain technologies, like gelatin for bone regeneration [32], or the utilization of gelatin in EBB [33]. Similarly, reviews dedicated to exploring the fabrication of particular tissues using specific bioprinting techniques, such as EBB for cartilage tissue [34] or VP for bone tissue [35], have been published.

However, there is currently a lack of comprehensive reviews focusing on the achievable resolution in 3D bioprinting.

The recent opinion article by Zandrini et al. [36] presents the latest advancements in high-definition 3D bioprinting, specifically focusing on clinical applications. In such work, the most cutting-edge results have been selected and reported, giving an insight on the recent achievements in the field.

The recent review from He [37] review presents interesting considerations about resolution in projection-based bioprinting, presenting both typical values of resolution and phenomena hindering the production of accurate structures.

In the current review, the authors aim to elucidate recent trends in 3D bioprinting, with particular emphasis on biomaterial utilized, technological advances and resolution attained across various 3D bioprinting technologies.

Given the rapid evolution of the field, authors chose not to apply any particular bias on final application, to ensure that the numerous studies in the literature focused on technological development and new materials were not excluded. All works aimed at the production of scaffold for tissue engineering or at biological patterning (therefore dealing with the processing of live cells) have been considered ab initio. Indeed, this review places emphasis also on works that achieve high resolutions through the optimization of process parameters, material composition, or the use of unconventional deposition strategies. This approach ensures a comprehensive evaluation of all relevant technologies, addressing both their development and application potential.

Technologies with lower typical resolutions are valuable for material development and can enhance performance when combined with specific strategies. Conversely, technologies with higher typical resolutions are generally closer to pre-clinical or clinical applications.

Therefore, it is essential to analyze materials suitable for different technologies, processing strategies, and the most commonly used characterization metrics, along with reporting the most advanced applications.

Together with these considerations, this work takes into account that the resolution alone is not sufficient for the achievement of clinically relevant results. Indeed, technologies have specific limitations hindering their applicability to regenerative medicine, which will be highlighted throughout the analysis.

Specifically, this work seeks to address two main research questions.

1. RQ1: "What are the state of the art and the current trends in the field of high-resolution 3D bioprinting?" From this primary research question, two additional sub-questions have emerged:
   - RQ 1.1: How prevalent are the various 3D bioprinting technologies in the current academic literature?
   - RQ 1.2: What are the bioink compositions compatible with each 3D bioprinting technology?

2. RQ2: How significant is the characterization of 3D bioprinting resolution in the literature, and what levels of resolution have been achieved for each technology?

In the following sections, the research methodology will be outlined, followed by the presentation of most valuable eligible works and aggregated data.

1.3. Literature selection methods

This literature review aims to detect and analyze all the trends in the field of 3D Bioprinting, considering materials used and resolution achieved. Many technologies have been highlighted, and each of them involves different material requirements and allows different levels of accuracy. The review was conducted by searching for works regarding all the aforementioned technologies. No specific constraints were imposed regarding resolution to avoid biases, as most instances of resolution characterization were expected to be found in articles covering broader topics. Consequently, the topic of resolution was successively analyzed across the search results to ensure inclusivity beyond articles explicitly focused on it.

The research was performed exploiting “Scopus” database as a repository for academic contents. Only research articles in English language belonging to a timespan ranging between 2017 and 2024 have been selected. As a matter of fact, the majority of case studies were found after 2017.

In order to select pertinent works, the following keywords have been used.

- “Bioprinting”, to define the context of research;
- “Cells”, in order to restrict results to articles involving the handling of biological materials, which increases the level of constraints compared to the use of bioink materials alone;
- A third keyword referring to the specific technology, in order to select all and only the aforementioned technologies.

Table 1 reports a complete list of keywords and constraints used to search for articles to be analyzed in the present review.

The exact research string used on the database is as follows: TITLE-ABS-KEY ("bioprinting" AND “cell” AND ("direct ink writing" OR "extrusion" OR “inkjet” OR "lift" OR "laser induced forward transfer" OR "vat" OR "stereolithography" OR "dlp" OR "lcd" OR "tpp" OR ″2pp" OR "two photon")) AND PUBYEAR >2016 AND PUBYEAR <2025 AND (LIMIT-TO (DOCTYPE, "ar")) AND (LIMIT-TO (LANGUAGE, "english"))

Among the results, a subgroup has been selected for quantitative evaluation by applying two eligibility criteria. The first criterion is the presence of clear characterization regarding the resolution or accuracy of printed construct, fabricated using animal cell-laden inks. Such requirement is needed to narrow down the results to the pertinent ones, according to the aim of the present work.

Table 1
Keywords, constraints and eligibility criteria used for literature research and selection used in the present review.

Database	Scopus
Document type	Research articles
Language	English
Year	2017 to 2024
Keyword 1	Bioprinting
Keyword 2	Cell
Keyword 3 (one among listed)	Extrusion, Direct Ink Writing, Inkjet, Laser Induced Forward Transfer, LIFT, Vat, Stereolithography, DLP, LCD, Two Photon, TPP, 2PP
Eligibility criterion 1	Characterization of resolution/accuracy
Eligibility criterion 2	Resolution smaller than 250 μm

The second criterion is the use of a setup enabling a resolution smaller than 250 μm. This criterion is necessary to further refine the selection of articles based on the quality of experimental results. Although this criterion does not impact studies involving light-based technologies (such as LIFT, VP, and 2PP), as their typical resolution is well below such threshold, it proves useful in excluding works related to EBB and inkjet achieving lower resolutions. However, these excluded works may still offer valuable insights aside from this specific topic, which are not considered of primary importance to this particular review.

Operationally, such second criterion can be translated in the use, by authors of research articles, of nozzles smaller than 250 μm or specific strategies able to produce features smaller than the threshold value. In this perspective, works based on the use of handheld dispensing systems have been excluded as well, since the manual deposition lacks repeatability even when small nozzles are employed.

The selection of works satisfying both eligibility criteria required full-text assessment because not all the studies clearly described their methods in abstracts.

In order to have a better insight on the selected works, they have been organized into clusters basing on the technology employed, and relevant data (which may vary depending on the specific technology) has been extracted from each of them.

2. Results and discussion

2.1. Reviewed literature

2.1.1. Extrusion-Based Bioprinting

EBB is the most utilized technology, with the majority of articles exploiting it for the production of bioprinted structures. The resolution achieved by this technology is lower when compared with light-based of jet-based methods, but its versatility and ease of implementation are at the base of its widespread adoption.

Indeed, many examples of non-traditional extrusion strategies have been found in literature. For example, works from Liu [38], Wang [39] and Tang [40] from 2018, 2019 and 2023, illustrate the use of coaxial nozzles for the fabrication of hollow tubular structures. In the second case, a gelatin/GelMA bioink has been printed into a cold bath and subsequently photo-crosslinked, allowing the production of hollow tubes with an inner diameter equal to 250 μm. In the latter case, the enzymatic crosslinking of GelMA, directly deposited into a viscous bath, allowed the fabrication of pipes with inner diameter and wall thickness as small as 70 and 4 μm, respectively.

Earlier, in 2018, Pi [41] published the design of a 3-shell coaxial nozzle, allowing the production of two-layered hollow pipes with an inner diameter of 600 μm and wall thicknesses of 60 and 100 μm.

Alternatively, different materials can be inserted in the same cartridge by means of a mold, as demonstrated by the two works from Kang [42,43], in order to produce multi-material extruded strands (Fig. 2c), with features as small as 30 μm, which can be particularly helpful in the obtainment of finely-vascularized tissues.

Bolivar-Monsalve adopted a similar methodology, publishing two studies [45,46], in 2021 and 2022, proposing the use of static mixer to create bi-material structures featuring perfusable micro-channels and lamellae with a thickness smaller than 50 μm (Fig. 2b), which allowed the easy circulation of culture media and therefore the effective cultivation of cells in relatively thick strands.

Due to the relative freedom in bioink formulation when exploiting EBB, functionalization of existing biopolymers is often performed to improve their printability of biological activity.

In 2019, Sarker [47] characterized the printability of peptide-conjugated alginate, which shows superior cell attachment capabilities, obtaining grids with a Pr (index related to the accuracy of grid-like structures) value equal to 1, while Kiyotake [48] developed a bioink based on pentenoate-functionalized hyaluronic acid and

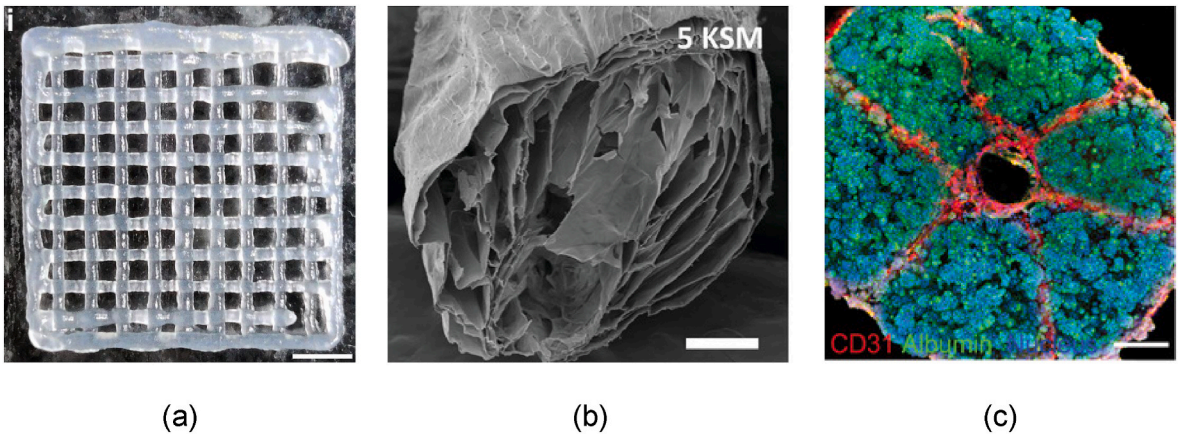

Fig. 2. (a) Grid printed using starch-based bioink, scale bar: 2 mm [44]; (b) Strand with internal lamellae and perfusable channels printed by using a static mixer as nozzle, scale bar: 200 μm [45]; (c) Strand with internal lobules obtained by inserting a mold inside the cartridge prior printing, scale bar: 200 μm [42].

dithiothreitol, obtaining extruded filaments of 450 μm.

To improve the printability of hydrogels, increasing their viscosity can be a viable option: the addition of gellan gum to GelMA by Zhuang [49] and of iota-carrageenan to silk fibroin by Moon [50] increased both the viscosity of the hydrogel and its printability, proving the effectiveness of such strategy. Both obtained spreading ration or line widths lower than the corresponding control compositions.

A similar approach has been followed by Ng in 2023 [51], who formulated a bioink based on gellan gum and pregelatinized starch, obtaining a spreading ratio (index related to the accuracy in the thickness of extruded filaments) equal to only 1.09 when using 27G nozzles.

In 2024, starch has been used by Shyam [44] as well, obtaining grids with a Pr value close to 1 when using 27G nozzles (Fig. 2a).

The rheology of bioinks is frequently tuned by adding fillers that enhance viscosity and impart yield stress to the material. In 2023, Maciel [52] utilized Laponite for this purpose, adding it to a gelatin/PVA-based bioink, which improved rheological properties and enabled the printing of grids with a Pr value of 1.05 and a strand width of 400 μm. Similarly, in 2024, Davern [53] employed Laponite in a GelMA-based hydrogel, achieving a strand width as small as 300 μm.

Cellulose serves as an excellent filler for EBB due to its biocompatibility and biodegradability. Notably, Gantumur [54] and Temirel [55]

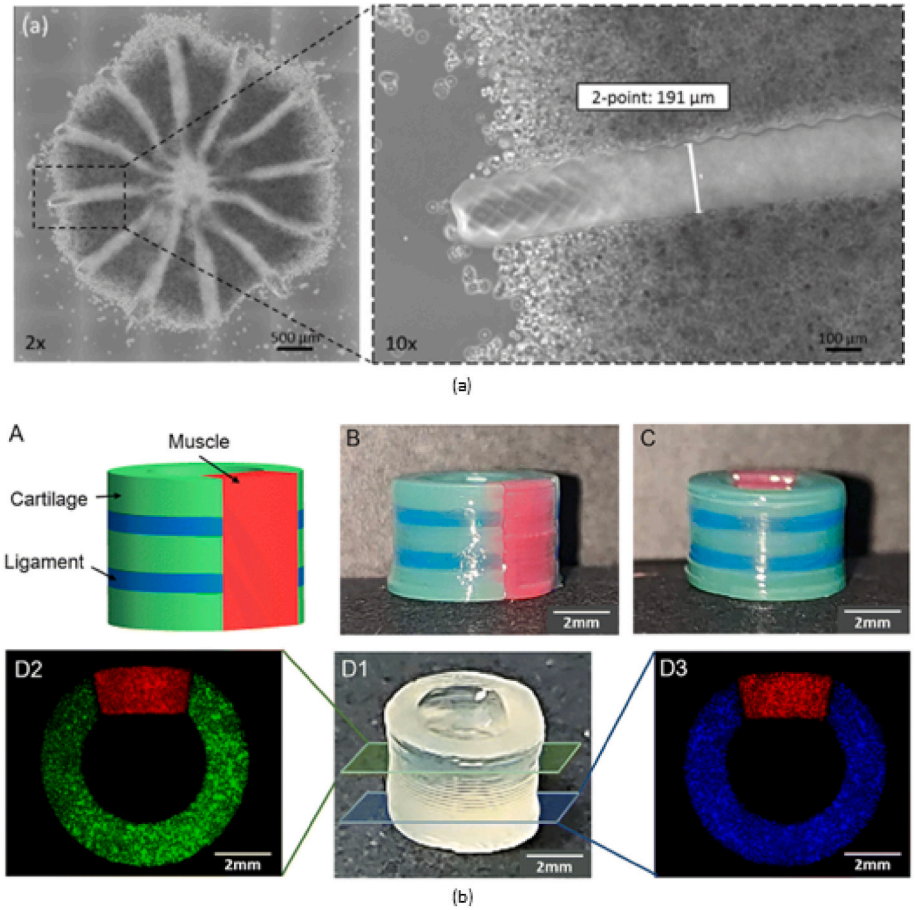

Fig. 3. (a) Liver Equivalents for Advanced Organ-on-a-Chip Applications [61]; (b) Multimaterial structure fabricated using a custom DLP setup [62]

utilized cellulose nanofibers and nanocrystals, respectively, in alginate-based bioinks, achieving extruded filaments as thin as 300 μm.

Another type of filler used in the literature is bio-based nanofibers. Specifically, Prendergast [56] and Sakai [57] employed norbornene-functionalized HA and silk fibroin nanofibers, achieving line widths of 200 and 400 μm, respectively. Prendergast particularly observed that the presence of nanofibers during extrusion resulted in better cell orientation.

Finally, together with experimental work, modelling and prediction proved to be an effective way to improve the resolution of bioprinted constructs.

Finally, in 2023, Hibbert [58] followed a systematic approach to find optimal parameters and improve printability of an alginate solution printed into a $CaCl_2$ bath. In this way, grids with Pr values of 1 and constructs with an integrity (index related to the accuracy in the height of three-dimensional structures) value of 0.99 were obtained.

2.1.2. *Vat photo-polymerization*

VP is the second most widespread technology in the field of 3D bioprinting, enabling the production of relatively small features and offering higher throughput compared to jet-based technologies. Currently, three different types of VP are in use: SLA, DLP, and LCD, each of which was previously explained in detail.

In the literature, the characterization of resolution in VP has been performed using various metrics, which often depend on the type of item printed.

Often, the width of rectilinear features is considered: the work from Sakai [59], in 2018, reports the fabrication of grids through DLP using an alginate derivative with a width of 500 μm, while Kumar [60] achieved a width of 250 μm using GelMA-based bioinks.

In 2018 Grix [61] published the fabrication of a liver organoid using a GelMA/PEGDA hydrogel through DLP, with walls as thin as 191 μm (Fig. 3a).

In case circular structures are printed, the characteristic diameter is usually reported: Xie [63] printed pores and cylinders with a diameter of 200 μm exploiting a bioink containing GelMA and cartilage extracellular matrix.

Alternatively, if hollow cylinders are printed, the achievable wall thickness can give a reliable insight on resolution of the process. Ma [64], in 2022, printed hollow cylinders with GelMA and PEGDA bioinks and achieved wall thicknesses of only 10 μm.

Cylindrical features can also provide an opportunity to characterize the vertical development of structures. By measuring the integrity, defined as the ratio of the actual height to the nominal height, one can obtain a reliable description of a material's suitability for VP-based processes. In 2023, Torras [65] reported the design and fabrication of an intestinal microenvironment printed using GelMA and PEGDA, with villus structures showing an integrity value as high as 0.9.

Notably, Duong [66] in 2023 published the optimization of process parameters for the production of branched multi-directional channels using norbornene-modified gelatin. Due to the complexity of the structure, the level of accuracy reached has been expressed as a function of the inner diameter of channels and of the actual perfusable length with respect to the nominal one: channels with diameters ranging between 300 and 1200 μm have been produced, with a perfusable length not lower than 80 % the nominal one.

An alternative option to express the resolution achieved by the printing process is to evaluate the shape fidelity factor of printed features: for instance, Choi [67] printed grids and scaffolds for artificial skin exploiting glycidyl methacrylate-grafted silk fibroin and gelatin, obtaining square pores featuring an SFF up to 1.

Often, proofs of concept are demonstrated by printing complex shapes such as ear replicas or other organs. In these instances, the evaluation of achieved resolution is qualitative and considers the accuracy of the printed structure relative to the nominal geometries. In 2022, Lee [68] fabricated replicas of various body parts, including the ear and brain using a bioink containing fluorescent silk fibroin, producing centimeter-scale structures with high accuracy.

When considering LCD, the achieved resolution is generally lower than that achieved with DLP. Chang [69], in 2022, reported the fabrication of channels with an inner diameter of 700 μm, while Wu [70], in the same year, printed grids with square pores of 500 μm and a wall thickness of 200 μm. However, Pérez-Cortez [71] in 2023 printed parts containing pores as small as 100 μm with an accuracy equal to 0.95 using GelMA-based hydrogels.

On the other hand, SLA achieves higher resolutions compared to DLP. In 2021, Zhang [72] published a study where GelMA was printed via SLA, resulting in pores of 100 μm. In 2022, Viray [73] reported fabricating scaffolds using poly(L-glutamic acid) with printed lines as thin as 8 μm. This represents the highest resolution achieved with VP-based technologies and cell-laden materials to date.

Alongside studies focused on developing new materials or optimizing printing parameters, some articles address overcoming the inherent limitations of VP technology. A significant limitation of VP is the lack of widely adopted systems for producing multi-material parts in a single printing process. To address this, some research efforts in the literature aim to enable this capability by designing new setups. Indeed, Su [62] and Grigoryan [74] presented multi-material DLP printers, achieving features as small as 250 μm (Fig. 3b), while Bhusal [75], in 2022, introduced a similar setup capable of producing grids with 15- μm pores.

Finally, the work from You [76] tries to overcome the scattering effect that cells can have inside a bioink when present in high densities, achieving a resolution as high as 50 μm

2.1.3. *Inkjet*

Inkjet is less widespread in 3D bioprinting with refer to EBB and VP, due to many limitations in the variety of suitable materials and producible structures.

In inkjet bioprinting, low viscosity materials are deposited onto a substrate as droplets, allowing the development of biological structures in a scaffold-free approach.

Indeed, one of the most used metrics for the quantification of resolution is the droplet size.

In 2020, Masaeli [77] reported the fabrication of multilayered heterocellular structures, characterizing both the droplet volume during flight (300 pL) and their diameter after deposition (629 μm). In the same year, Masaeli [78] also published a study on producing an in vitro retina model using inkjet printing, depositing 300 pL droplets, each containing an average of 93 cells.

The measurement of the number of cells per drop is a rather common practice in inkjet bioprinting, indeed, in the works from Takagi [79] and Park [80], droplet containing between 0 and two cells each are deposited, while in a successive work from Park [80] and in the one from Dudman [81], single cell deposition is achieved.

Finally, the fabrication of more complex structured is reported as well: Hewes [82], in 2017, reported the fabrication of microvessels with an inner diameter of 300 μm, depositing droplets of alginate solutions in a $CaCl_2$ bath. In the same year, Compaan [83] published the printing of tubes with a diameter of 5 mm and a wall thickness of 400 μm using a bioink containing silk fibroin and alginate.

2.1.4. *Laser induced forward transfer*

Most works exploiting LIFT are focused on the optimization of printing parameter in order to achieve effective transfer towards the substrate.

As a consequence, the usual characterization for the evaluation of resolution is the resulting diameter of deposited droplets.

In 2017, Koch [84] studied the effect of various printing parameters (including wavelength and laser pulse duration) in the deposition of an alginate/EDTA blood plasma bioink, achieving droplets as small as 100 μm.

More recently, Shakil [85] published a work in which different

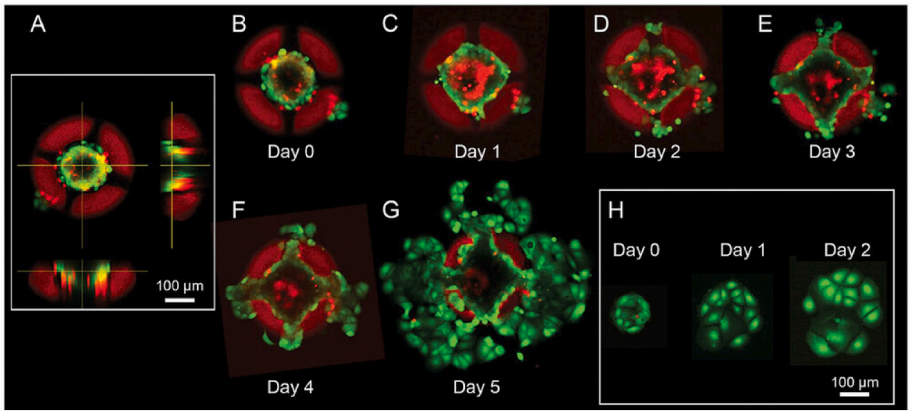

Fig. 4. Confinement structure for cell spheroids printed by 2PP using gelatin based commercial ink [91].

configurations of bioinks were tested and analyzed through design of experiment, managing to deposit both single droplets and continuous lines.

The only work eligible for this review exploiting LIFT for the production of complex structures is the one from Xiong [86]. In such work, alginate is deposited using gelatin as an energy absorbing layer, producing straight and branched tubes with diameters equal to 3 mm.

2.1.5. *Two-Photon Polymerization*

2PP is the 3D bioprinting technology that enables the highest level of resolution, surpassing all other existing techniques in its ability to produce extremely fine and intricate structures.

In 2020, Urciuolo [87] published a work about intravital bioprinting, in which hydrogels are printed across and within tissues of live mice. Such technique enables the fabrication of complex structures inside tissues of live mice, with the possibility of producing lines with a thickness equal to 1.9 µm and a spacing of only 0.5 µm.

In the same year, Tytgat [88] printed bioinks containing norbornene and thiol-functionalized collagen or methacrylamide-functionalized collagen, obtaining features as small as 20 µm. Similarly, Dobos [89] used norbornene-modified gelatin and thiol-modified gelatin to formulate a bioink for the production of micro-channels with inner diameter of 30 µm.

In 2022, Valente [90] published a work about the printing of silk fibroin hydrogel with directly tunable physico-chemical properties. 2PP allowed control of the crosslinking degree, the porosity of the resulting hydrogel and the degradation rate. Both large and small-scale structures were obtained for with a good degree of accuracy.

The work from Taale reports the fabrication, through 2PP, of confinement structures surrounding tumoral cell spheroids (Fig. 4), in order to study complex phenomena involved in cancer progression, such as the diffusion through confined structures. For this scope, hollow spheres with a diameter of 260 µm and a wall thickness of 50 µm were constructed around cell spheroids, featuring pores as small as 20 µm.

Finally, Rizzo, in 2023, published a work in which hyaluronic acid maleimide has been used to produce features as small as 1 µm.

2.2. *State of the art and trends in 3D bioprinting*

A preliminary answer to RQs can be retrieved by having an overview over research results and academic works selection. Fig. 5a shows the distribution of research articles corresponding to search keywords published from 2007 (the earliest year of results found) to February 2024. The total number of works gathered is 1247. The temporal restriction imposed (articles published from 2017 onwards) led to the inclusion of 90.3 % (945) of the total results in the research dataset, confirming that such limit included the majority of available works.

Bioprinting, despite nearly 20 years of progress, is still in an exponential growth phase due to the ongoing challenge of printing large-scale tissues and fully functioning organs. Active research continues to explore new materials, technological advances, and strategies for improvement.

Fig. 5b outlines the steps used to apply eligibility criteria and select results for analysis. Over 20 % of the works met criterion 1, indicating that resolution remains a key focus, reflecting the field's aim to mimic highly complex systems. Resolution is essential for precise control of intricate structures involving multiple materials.

For criterion 2, only about 10 % of works met the quantitative

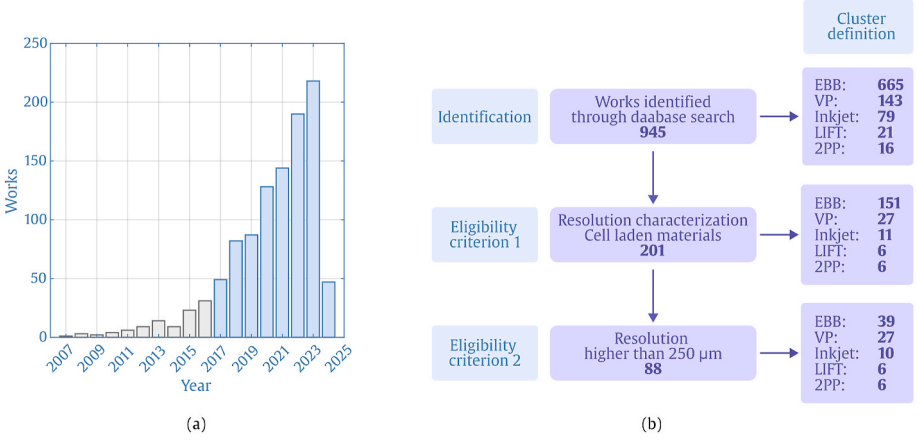

Fig. 5. (a) Articles published per year, selected using keywords from the research string. (b) Diagram of steps performed for article selection.

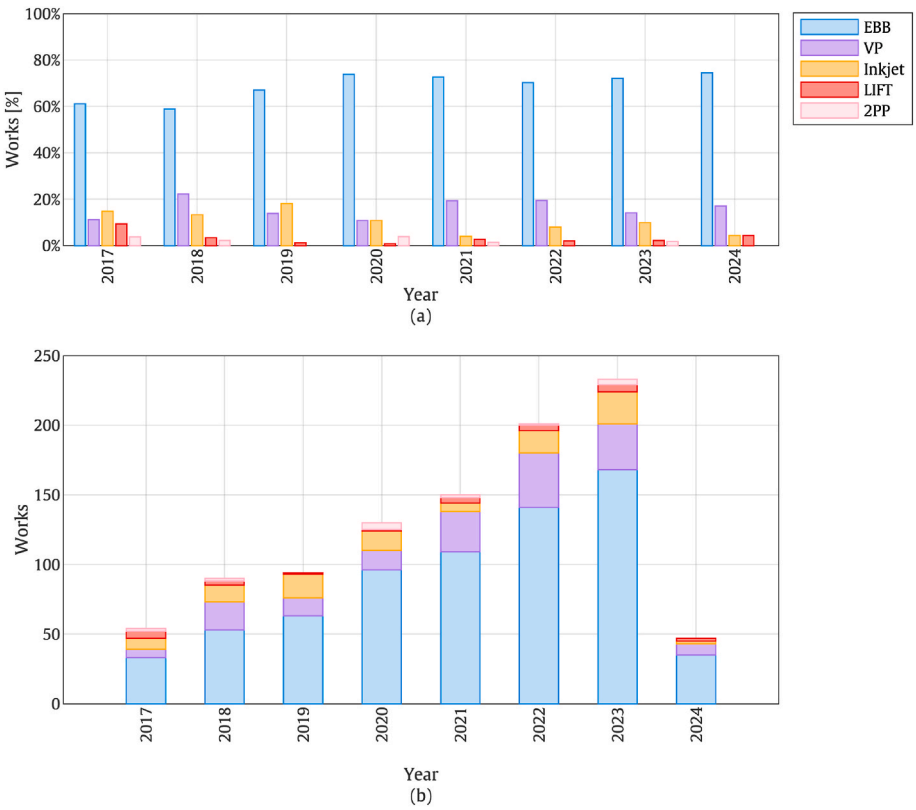

Fig. 6. (a) Percentage of published articles per technology between 2017 e 2024; (b) Number of published articles per technology between 2017 e 2024.

threshold, suggesting further research is needed despite significant advances in materials and technologies.

In summary, the field of 3D bioprinting is experiencing increasing interest and growth in research, as shown by the statistics regarding academic publications and reflecting its exponential growth phase. Together with the development of materials and technologies able to sustain cell growth and functional tissue development, resolution is an important aspect to be considered in advancing the field and to allow the production of complex systems, with its characterization present across numerous works. While the achieved levels of resolution are promising, further research is necessary to ensure more works meet targets needed for the production of complex and functional structures.

To gain a deeper insight into 3D bioprinting trends and better address RQ1.1, it is useful to analyze published articles by technology (Fig. 6a and b). The most prevalent method is EBB, used in over 60 % of articles annually, with both its percentage and the total number of articles steadily increasing. This dominance is due to its simplicity, similarly to FDM 3D printing, making it accessible even to researchers with limited additive manufacturing experience. Additionally, EBB-based bioprinters have been widely available for nearly a decade and are more cost-effective than setups like SLA, LIFT, or 2PP.

Material formulation for EBB is also easier compared to other technologies, allowing the use of various biopolymers at higher concentrations. EBB accommodates a wider viscosity range than inkjet printing and offers higher throughput than inkjet, LIFT, and 2PP, while requiring less material than VP. Its ability to quickly fabricate centimeter-scale structures is crucial for cell-laden materials, helping prevent issues like cell sedimentation and death. Furthermore, EBB ensures efficient use of materials by only utilizing what is necessary for the final structure.

VP is the second most used technology, with a stable percentage over the years but an overall increase in published articles (Fig. 6a and b). This rise in interest is largely due to the introduction of DLP- and LCD-based 3D printers, which offer resolutions of just a few tens of microns and significantly higher printing speeds and lower price compared to traditional SLA machines.

For VP-based 3D bioprinting, material formulation is less constrained since there is no need for the material to flow through a nozzle or be ejected. This reduces the rheological limitations and minimizes the shear stress on cells, decreasing the risk of cellular damage—a common issue with EBB processes. However, the need for a vat to hold the material to be photopolymerized requires using more material than necessary for the final structure, requiring more biological material and complicating multi-material printing, despite some custom solutions [62,74,75].

DLP and LCD printers, which can crosslink entire layers at once (unlike EBB and SLA's pointwise addition), help reduce overall printing time, offering an optimal balance between speed and resolution for centimeter-scale structures.

Inkjet technology, the first used for automated dispensing of cell-laden materials [92], initiated the field of 3D bioprinting but has seen limited use in recent years (Fig. 6a and b). While the number of articles on inkjet bioprinting has grown with the field, its share has decreased, surpassed by VP since 2021.

This decline is linked to the strict rheological requirements: ink viscosity must be low for controlled deposition, limiting material choices to low-concentration hydrogels or aqueous media. As a result, only nearly two-dimensional structures can be fabricated, making inkjet less suitable for 3D scaffolds. Additionally, its low throughput leads to long printing times for large structures, risking cell sedimentation, nozzle clogging, and dehydration.

Process optimization is complex due to factors like deposition waveform, nozzle diameter, feed rate, and substrate characteristics, which must also account for cell viability. Moreover, process characterization relies on optical analysis of droplets in flight, requiring sophisticated and expensive equipment to capture microsecond-scale

events.

LIFT is a promising but still underexplored technology for 3D bioprinting, with only a small number of publications on its use with cell-laden materials (Fig. 6a and b). Unlike more established methods like EBB, VP, and inkjet, LIFT is relatively new in 3D printing, especially for bioprinting, and presents technical challenges.

Most studies focus on optimizing parameters for precise drop deposition, leaving large-scale 3D structure fabrication for future research. Laser-cell interactions and the mechanical stress during material transfer are areas of concern, as they could harm biological materials.

Like inkjet, LIFT imposes strict constraints on the rheological properties of materials, limiting viable options. Additionally, the need to deposit a thin layer of material on the donor substrate increases the risk of dehydration, especially with the long printing times and low throughput, making it difficult to produce large scaffolds. The high cost of the required laser, optical, and positioning systems further limits LIFT's widespread adoption.

The final technology within the realm of 3D bioprinting is 2PP, renowned for achieving extremely high resolutions, down to just a few microns. However, like LIFT, its use is still limited, with few articles published in recent years (Fig. 6a and b). This is largely due to its relative novelty and the higher costs involved compared to more commonly used methods.

Material availability is also a challenge. The distinct photopolymerization mechanism used in 2PP makes developing new materials a primary research focus. Additionally, the printing process occurs within a droplet of photocurable resin, limiting the size of structures and the volumetric throughput, which restricts its application for large-scale scaffolds.

Despite these limitations, 2PP has shifted the 3D bioprinting paradigm by enabling precise manipulations at the cellular level. It can be used to create solid barriers within developing tissues [93] or attach hydrogel parts to individual bacteria [94], allowing for the tracking and monitoring of single cells.

To briefly summarize the answer to RQ1.1, the main key points are listed following.

- EBB dominates 3D bioprinting, with its simplicity and cost-effectiveness driving its widespread adoption. Its formulation flexibility and high throughput make it favorable for rapid fabrication of structures, especially crucial for cell-laden materials, while minimizing material waste.
- VP technology, ranking second in usage, shows stable percentages and a rising number of articles. Its advantages are based on high resolution, high printing speed, and cost-effectiveness. Despite fewer material constraints and reduced cellular stress, challenges remain in excessive material usage and multi-material bioprinting.
- Inkjet, the first automated cell-laden material dispensing technology, has seen reduced usage lately, overtaken by VP since 2021. Constraints on ink viscosity limit material options and structural complexity, leading to low throughput and process optimization challenges. Optical analysis of drop formation requires costly systems, adding complexity.
- LIFT shows potential for 3D bioprinting but faces technical challenges in handling cell-laden materials and fabricating large, complex structures. Issues include optimizing drop deposition, laser-cell interaction, material rheology constraints, material dehydration, high apparatus costs and limited throughput.
- 2PP, renowned for its high-resolution capabilities, faces limited publication due to its novelty, higher setup costs and materials availability. Due to its process occurring within a drop of resin, structural size and volumetric throughput are limited, unsuitable for large-scale scaffolds. However, 2PP enables precise manipulation of single cells, marking a shift in 3D bioprinting towards cellular-level control.

2.3. Bioinks composition

RQ1.2 can be answered by considering the materials used in articles satisfying both eligibility criterion (Fig. 7a). Numerous materials are

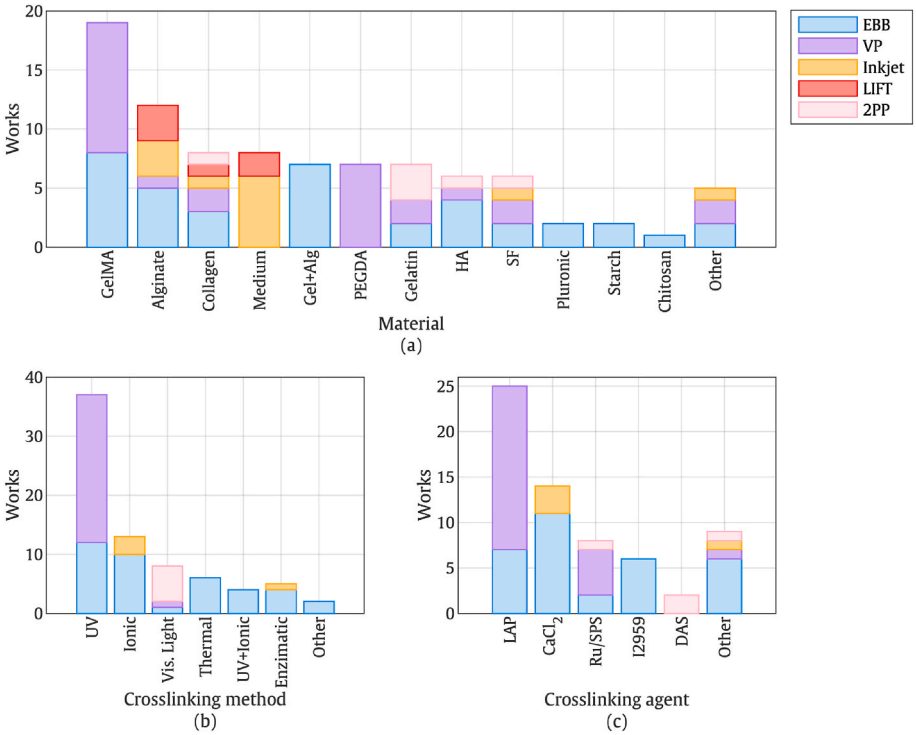

Fig. 7. (a) Materials used in 3D bioprinting in eligible articles; (b) Crosslinking methods used in 3D bioprinting in eligible articles; (c) Crosslinking agents used in 3D bioprinting in eligible articles.

available for 3D bioprinting, primarily water-soluble polymers, often of biological origin, which undergo crosslinking either during or after printing.

The most used material is gelatin methacryloyl (also known as methacrylated gelatin or GelMA). It is widely used because of its tunable mechanical properties, high biocompatibility and biodegradability, cell proliferation properties and availability [3].

GelMA is a synthetic polymer obtained by functionalizing gelatin with methacrylic groups, which make it suitable for photo-crosslinking [3].

Basing on the considered publications, it is particularly used in EBB [39,40,46,49,53,56,95,96] and VP [60,61,63,64,65,67,71,72,97–99] in the form of hydrogels typically containing 5–10 % GelMA. Indeed, uncrosslinked GelMA hydrogels show sufficient viscosity, shear-thinning and Bingham-like behaviour at room temperature, allowing extrudability and shape retention of produced structures and making it particularly suitable for EBB. Usually, GelMA is photo-crosslinked during the printing process (e.g. at the end of each layer) or in a successive moment.

If kept at 37 °C, GelMA hydrogels are in the liquid state, showing a lower viscosity which, together with the suitability for photo-crosslinking, makes it suitable for VP.

The rheological properties of GelMA and its spontaneous gelation at room temperature make it hardly suitable for inkjet and LIFT, for which it could be used only at very low concentrations.

Alginate is a widespread and versatile polymer for 3D bioprinting. It is a natural polysaccharide extracted from marine algae which shows all biological and mechanical properties listed for GelMA. It can be physically crosslinked by contact with bivalent cations, such as Ca^{2+} ions present in $CaCl_2$ solutions, or chemically modified in order to make it suitable for photo-crosslinking [3].

Due to the absence of spontaneous gelation and low viscosity of alginate solutions, such material is successfully used in EBB [38,47,54,55,100] VP [59], Inkjet [82,83] and LIFT [84,86,101].

As regards EBB, alginate solution cannot guarantee shape retention, therefore in this case it has been used together with secondary polymers or fillers needed for the scope [54,55,100]. Alternatively, it has been directly printed into a $CaCl_2$ bath [38], or as sacrificial core material in coaxial printing [46].

The third most used material is collagen, a natural-occurring protein which is found in the connective tissue of all mammals. Being a naturally occurring polymer, excellent biological and mechanical properties are shown by collagen-based scaffolds [3]. Despite its limited solubility in water and slow gelation rate (taking place by heating the hydrogel at ≈37 °C), it is successfully used in many technologies. Indeed, it can be used in small percentages, obtaining low viscosity solutions suitable for inkjet printing [102], while higher-percentage solutions are successfully used in EBB [42,43,103] thanks to its high viscosity which favors shape retention.

Collagen can be variously functionalized in order to make it suitable for light-based technologies. Indeed, methacrylated collagen has been successfully employed in VP [70,97], while norbornene, thiol-and methacrylamide functionalized collagens have been exploited for 2PP.

Aqueous culture media can be used in 3D bioprinting in a scaffold-free approach: cells are deposited following precise patterns and self-aggregation is exploited for the formation of tissues, in a process mimicking embryonic development [3]. Obviously, aqueous culture media do not offer any possibility for photo-crosslinking nor shape retention, therefore they are not suitable for EBB and light-based processes. They have been employed in inkjet [77–81,104] and LIFT [105,106], due to their very low viscosity, allowing a proper formation and transfer of droplets. This way, two-dimensional structures can be formed, lacking the possibility to stack numerous layers, but allowing to deposit droplets containing even single cells.

A commonly utilized class of hydrogels in 3D bioprinting is gelatin (or its modified forms) combined with alginate, offering a blend of their individual properties while enabling finer adjustment of mechanical characteristics. With alginate, ionic crosslinking is feasible, and when GelMA substitutes gelatin, UV curing becomes an option, enhancing versatility. This hydrogel class has been effectively employed in EBB (Fig. 7a) applications, utilizing both gelatin [107–109] and GelMA [41,45,110,111].

Polyethylene glycol (PEG) is another prevalent polymer in 3D bioprinting, valued for its water solubility, favorable printability in EBB, adequate mechanical properties and tunable molecular weight. However, its biological inertness, lacking naturally occurring functional groups, prohibits cell adhesion, thereby hindering the development of functional tissue [3].

Its modified form, Polyethylene glycol diacrylate (PEGDA), can undergo photocrosslinking, making it a suitable material for light-based applications.

Among articles selected for the current review, it has been exploited in VP, both mixed with bioactive components [75] or alone, in order to explore the potential of the technology and the design of complex structures [62,69,112–114].

Alternatively to GelMA, gelatin, either in its pristine form or in modified versions, is exploited as a constituent for bioinks due to its favorable properties. It is utilized in EBB to explore the effects of innovative fillers [52] and in the form of UV-curable norbornene-functionalized gelatin for scaffold fabrication [115]. This version of gelatin is also applicable in VP [66], while combinations like gelatin with PEGDA enable photocrosslinking [116]. In 2PP, modified gelatin variants are the preferred option for photocrosslinking using visible light [87,88,89].

Hyaluronic acid (HA), a linear non-sulfated glycosaminoglycan, is ubiquitous in almost all connective tissues and a major ECM component of cartilage. It behaves similar to collagen, showing excellent biocompatibility and ability to form flexible hydrogels. Also HA can be chemically modified to make it photo-crosslinkable or to improve its properties [3].

Modified forms of HA have been used in EBB [57,117] to develop innovative hydrogels, while its photo-crosslinkable version find applications in EBB [48,118], VP [119], and 2PP [120].

While other polymers such as silk fibroin (SF) [50,67,68,90,121], Pluronic F-127 [58,122], starch [44,51], and chitosan [123] have found applications in 3D bioprinting, their discussion is relatively limited here. This is primarily due to their poorer typical properties or challenges encountered in their processing, leading to their decreased statistical relevance within the scope of this review.

Regarding crosslinking methods, the options vary based on the bioink composition and technology employed. While light-based techniques necessitate photo-crosslinking, extrusion or jetting processes offer a wider array of possible mechanisms including ionic, thermal, and enzymatic crosslinking [3]. The choice of crosslinking agent follows the selected mechanism, with photo-initiators required for photo-crosslinking, salts serving as ionic precursors, and specific enzymes facilitating enzymatic crosslinking.

Fig. 7b and c show the occurrences of different crosslinking mechanisms and crosslinking agents within the articles selected for the review.

Photo-crosslinking is the most commonly utilized mechanism. Depending on the technology and setup, three different wavelengths are the most used in literature: UV light at 365 nm, UV–Vis light at 405 nm and visible/infrared light between 700 and 1000 nm.

This approach offers superior spatiotemporal control, as it is faster and potentially more localized compared to ionic and enzymatic mechanisms, which somehow rely on the contact between two solutions and the diffusion of crosslinking agents into the structure. Furthermore, UV–visible light or, ideally, visible light (typical in 2PP) minimizes or eliminates undesired effects on cells, unlike, for example, the temporary osmotic equilibrium alteration and reduced cell viability that can result from using salts as ionic precursors.

In this context, the most used photo-initiators are Lithium phenyl-2,4,6-trimethylbenzoylphosphinate (LAP), ruthenium (Ru) + sodium

persulfate (SPS) and 1-[4-(2-hydroxyethoxy)-phenyl]-2-hydroxy-2-methyl-1-propan-1-one (mostly known by its commercial name Irgacure 2959 or as I2959), as shown in Fig. 7c.

Specifically, LAP is frequently favored for its excellent biocompatibility, water solubility, and its ability to produce hydrogels with finer and more durable microstructures. Its absorption peak is around 405 nm, making it particularly suitable for all commercial printer emitting light at such wavelength. [124] Thanks to its several advantages, LAP is the most used photo-initiator among selected articles and it is used both in EBB [39,46,53,56,95,110,115] and VP [61,62,64–68,70–72,75,97,98,113,114,116,119,125].

The Ru/SPS system is preferred over I2959 due to its less adverse effect on cells in long-term cultures and its significantly greater light penetration depth. Moreover, Ru/SPS is particularly suitable for visible-light photo-crosslinking applications. Indeed, it is used in EBB [50,121], VP [59,69,73,99,112] and 2PP [90].

On the other hand, I2959, despite its lower water solubility, possesses an absorption peak at 365 nm, making it the most suitable option for printers emitting light at this wavelength [126].

Due to its absorption peak at 365, I2925 is only used in EBB [38,40,48,49,111,118], being most commercial printers for VP based on a 405-nm light source.

As regards 2PP, it exploits a wavelength considerably different than the one typically used in VP. Indeed, the former exploits the range of red/near-infrared light (700–1000 nm), while the latter is based on UV–visible light (365–405 nm). As a consequence, the use of a different photo-initiator (tetrapotassium 4,4′-(1,2-ethenediyl)bis[2-(3-sulfophenyl)diazenesulfonate], DAS) has been found in literature [88,89].

Ionic crosslinking is particularly convenient when dealing with alginate, which almost immediately crosslinks in contact with solutions containing calcium ions. Indeed, calcium chloride is the most exploited crosslinker in EBB, where structures can be immersed in a $CaCl_2$ bath after printing [43,46,47,55,58,100,107–111].

In coaxial EBB, such solution can be used as a core sacrificial material, allowing to instantly crosslink the outer alginate shell to obtain hollow structures [38,41].

In inkjet printing, the most exploited crosslinking technique is to directly print alginate-based hydrogels into a $CaCl_2$ bath, in order to have immediate solidification of the droplet [79,82,83].

Thermal gelation is a viable option to obtain stable structures when dealing with materials like collagen, which crosslinks upon heating (rather than typical hydrogels, which solidify upon cooling), or when long term stability of the structure is not needed. Such mechanism is surely not suitable for light based technologies, but is present in a significant number of works on EBB [42,43,52,127].

Enzymatic crosslinking is the last class of crosslinking mechanisms found, which, similarly to ionic crosslinking, is based on the contact between the hydrogel and a solution containing the specific enzyme needed for solidification [54,57,128,129]. Also here, it is possible to have the structure immersed into the bath: in this case, due to the slow diffusion of enzymes into the structure, it is possible to obtain particularly thin hollow tubes, since the crosslinking only takes place in a superficial region and allows to remove the inner material [40].

It is noteworthy that articles on inkjet and LIFT typically do not report any crosslinking mechanism. These technologies frequently use aqueous media as a bioink, precluding the possibility of crosslinking the structure. Instead, they rely on cellular self-assembling in a scaffold-free approach. Additionally, in the case of LIFT, most articles focus on optimizing parameters for proper deposition and improvement of resolution, instead of the actual production of three-dimensional structures.

2.4. Resolution

To address RQ2, analyzing the trend of articles characterizing resolution in 3D bioprinting is informative. The number of articles on this topic has been increasing annually (Fig. 8a), reflecting a growing interest in achieving higher resolutions in line with the overall growth in the field. Despite advancements, the goal of producing complex, large-scale vascularized tissues remains unreached. Achieving a higher degree of spatial control in material deposition is crucial, with resolution being a key challenge.

Notably, the percentage of articles meeting the characterization criterion has surged since 2020 (Fig. 8b). While a single explanation is difficult to pinpoint, the publication of a significant review that year on

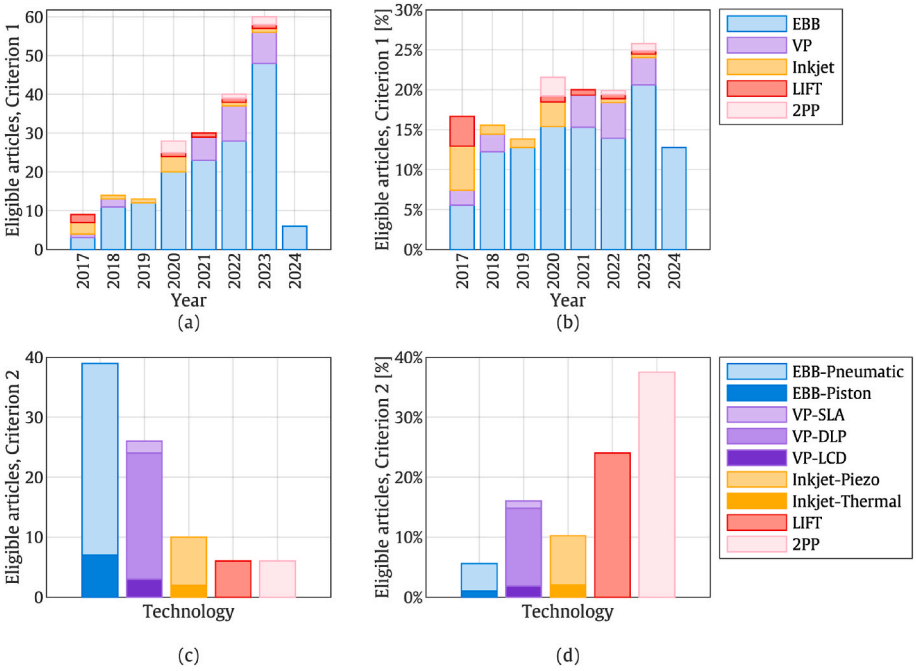

Fig. 8. (a) Number of published articles meeting eligibility criterion 1; (b) Percentage of published articles meeting eligibility criterion 1 relative to the total number of articles published per year; (c) Number of published articles meeting eligibility criterion 2; (d) Percentage of published articles meeting eligibility criterion 2 relative to the total number of articles published on each technology.

bioinks' rheological factors and printability [130] reflects the maturation of interest on the topic and the need for a thorough and systematic characterization protocol. Additionally, the emergence of high-resolution technologies like LIFT and 2PP has redefined resolution standards in 3D bioprinting, attracting attention across various technologies.

To evaluate the achieved resolution and address the final aspect of RQ2, we examine the percentage of articles meeting eligibility criterion 2: the number and percentage of articles capable of achieving a resolution below 250 μm based on the utilized setup, relative to the total published articles for each technology from 2017 to 2024 (Fig. 8c and d).

The number of articles with setups allowing resolutions smaller than 250 μm correlates with the total articles published for each technology, with EBB having the highest number of eligible articles, followed by VP, inkjet, LIFT, and 2PP. However, when considering the percentage of eligible articles, EBB shows the lowest percentage, indicating it is the least suitable for achieving high resolutions.

In contrast, VP boasts an eligible article percentage nearly three times higher than EBB, as VP technologies generally facilitate better detail across all variants. Notably, all articles characterizing resolution in VP met the second eligibility criterion, whereas only 39 out of 151 articles on EBB satisfied the resolution threshold.

As regards inkjet, 10 articles out of 11 characterizing resolution met eligibility criterion 2. Therefore, the lower percentage of works with respect to the published ones is not related to problems in achieving high resolution, but to challenges in the characterization of resolution. Indeed, as explained, the observation of ejected droplets relies on sophisticated and often expensive systems, hindering the characterization of the phenomenon.

Lastly, LIFT and 2PP exhibit a pattern similar to VP, where all articles meeting eligibility criterion 1 also fulfill the second criterion. This underscores a significant investigation into achievable resolution, likely stemming from the relative novelty of these technologies and the subsequent need for a deeper understanding of their control and potential, but also the possibility to achieve high levels of resolution in the majority of cases.

Throughout the selected works, resolution is quantified by using various metrics, which are reported in Table 2 and Fig. 9.

In bioprinting, resolution refers to the smallest distinguishable feature. However, depending on what features are considered, such as positive and negative features or horizontal and vertical orientations, the level of resolution can vary even with identical setups, materials, and printing parameters. These varying definitions and evaluation methods across studies complicate direct comparisons of results [37]. As a concequence, various metrics have been employed to express resolution, also reflecting the diverse underlying mechanisms of each technology.

Table 2
List of metrics used in literature to quantify resolution.

Variable definition	Description	Occurrences
$Pr = \frac{L^2}{16A}$	When printing grids in EBB, the pore index *Pr* describes how pores are close to ideal squares by considering the internal perimeter *L* and area *A* of printed pores.	12
$A = \frac{X_{actual}}{X_{nominal}}$	Accuracy A *A*: the ratio of the dimension of a printed feature X_{actual} to its nominal dimension $X_{nominal}$.	14
W	Strand width *W*, the average width of extruded filaments in EBB.	25
$I = \frac{h_{actual}}{h_{nominal}}$	Integrity *I*: ratio of height of the printed structure h_{actual} to its nominal value $h_{nominal}$.	3
SPF	Smallest printable feature.	29
$C = \frac{4\pi A}{p^2}$	Circularity *C* of printed pores, evaluated as a function of pore area *A* and perimeter *p*.	1
R_a	Average roughness of printed part	1
D_D	Droplet dimension	12
CN	Number of cells per drop	7

For instance, in inkjet and LIFT technologies, resolution is often quantified by the dimension of individual droplets during flight or upon deposition, emphasizing the precision of droplet placement. In contrast, EBB tends to measure resolution in terms of strand width or internal feature dimensions within printed structures (often square grids), highlighting the control over material extrusion. VP and 2PP technologies, on the other hand, focus on the finest achievable feature size, which underscores their capability for high-resolution, intricate designs.

While different technologies may require distinct metrics to express their resolution, the use of multiple metrics within each technology in the literature complicates comparisons between different works. Adopting unified metrics and a standardized protocol for each technology would promote better and easier comparisons, greatly benefiting scientists in the field.

Most metrics for evaluating resolution focus on the xy plane, with only one (integrity) addressing accuracy in the vertical (z) direction. This is largely due to the fact that z-direction resolution is governed by layer height, which depends more on the printing setup than on material or process optimization. While layer height is commonly reported as a printing parameter, the actual final height of constructs is rarely characterized. Layer heights as small as a few tens of microns are achievable with most technologies, particularly light-based methods, but controlling resolution in the xy plane remains the primary challenge due to construct spreading.

A final consideration must be made regarding the factors that limit achievable resolution, irrespective of the metrics used to define it. In EBB, for example, surface tension can impact corner precision [131]. In light-based technologies, dyes may enhance resolution through light confinement [113], while high cell density can cause light scattering [132,133]. Alternatively, variations in light focusing systems may result in poor resolution [101]. Although the nominal resolution of setups can often reach a few tens of microns or less, the actual resolution achieved must consider material responses and the limiting factors discussed [37]. Therefore, these limitations must be evaluated on a case-by-case basis

Fig. 10a illustrates the level of resolution achieved by the articles selected for this review. It is evident that 2PP, which is regarded as the technology with the highest resolution capabilities, consistently achieves a resolution of 50 μm or lower across all reviewed works. Notably, two studies report resolutions of 2 μm and 1.9 μm, respectively [87, 120].

Regarding LIFT, a satisfactory level of resolution is achieved, with results ranging between 80 and 250 μm. However, it is important to note that these studies primarily focus on the deposition of drops or lines rather than the fabrication of three-dimensional structures or complex geometries. This underscores that, while LIFT demonstrates promising potential as indicated by the achieved resolutions, further research is needed to advance the technology toward the production of more application-ready pieces.

A similar result is visible for what regards inkjet, which shows many resolutions ranging between 50 and 90 μm. However, these values often refer to the diameter of the droplet observed during its flight between the nozzle and the substrate. Only one work measured the actual diameter of droplets once they are deposited on the substrate [77], with an average value of 629 μm, and two measured printed features [82,83], with values of 300 and 400 μm, respectively. Therefore, it is reasonable to assume that the resolution achievable in fabricating complete structures with this technology is not as fine as what is reported by observing droplets during the flight only.

VP has more disperse values of resolution, which also result by the presence of three variants of the technology. When considering SLA, values as low as 8 μm have been achieved [73], while DLP allows to print with a resolution of 10 μm [64]. In the context of LCD printers, despite their affordability, they have only achieved resolutions up to 100 μm [71]. This performance is still comparable to the resolutions obtained with LIFT technology.

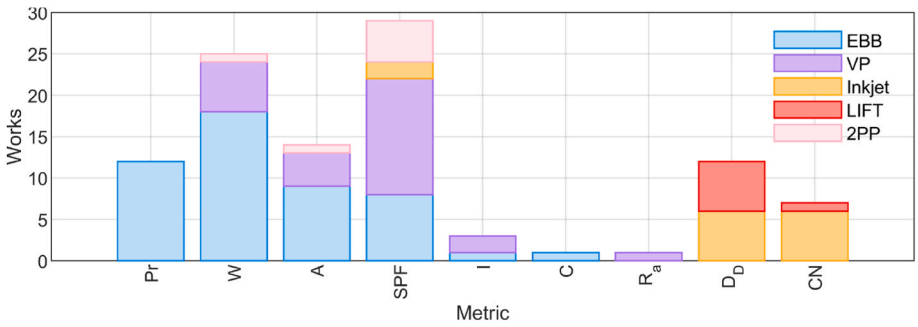

Fig. 9. Metrics used for the characterization of resolution in eligible articles.

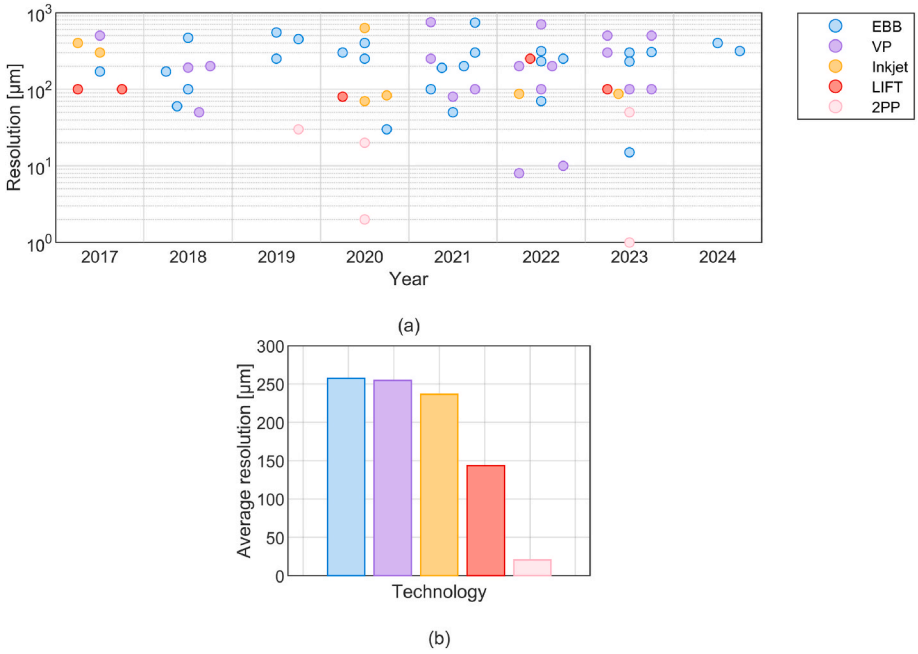

Fig. 10. (a) Resolution achieved by articles selected for the current review; (b) Average achieved resolution for the different technologies.

Finally, it is evident that EBB exhibits a wide range of resolution values. Some studies report unconventional strategies able to overcome average resolutions and achieving values as fine as few tens of microns. These advanced methods include using coaxial nozzles to produce fine wall thicknesses in hollow strands [40,41] or employing novel techniques such as static mixing of materials prior deposition [46] and inserting molds within cartridges [42]. Such novel techniques allow to produce strands showing peculiar internal microstructures. Regarding the width of entire strands, only one study achieved values as low as 70 µm [127], while the average resolutions are generally higher than 250 µm.

Looking at the average values achieved by the technologies (Fig. 10b) generally gives a reliable insight for what regards for what regards VP, LIFT and 2PP. For inkjet, the results should be interpreted with caution due to the lack of characterization of deposited droplets.

A similar reasoning applies to EBB: the results include studies characterizing features within single strands and exclude works using nozzles larger than 250 µm. This skews the average resolution of EBB to similar to VP, which is evidently misleading. In fact, only 7 out of 151 works (4.6 %) characterizing resolution in EBB achieve a resolution below 100 µm, whereas in VP, 8 out of 26 works (30.7 %) meet this threshold.

3. Conclusions and future perspectives

This review selected the most relevant works in the rapidly evolving field of 3D bioprinting to analyze technological trends, materials, and the levels of resolution achieved across a range of studies. The primary technologies examined include Extrusion-Based Bioprinting (EBB), Vat Photopolymerization (VP), Inkjet, Laser-Induced Forward Transfer (LIFT), and Two-Photon Polymerization (2PP), each with its own strengths and limitations.

EBB is the most widespread technology, favored for its versatility, ease of implementation, and high throughput, despite having limited resolution. This makes it particularly suitable for applications that require larger constructs, such as scaffolds for tissue engineering in regenerative medicine. VP, on the other hand, offers a better balance between throughput, characteristic dimensions, and resolution, positioning it as a key technology for applications where fine detail and controlled geometry are important.

In contrast, jet-based technologies like Inkjet and LIFT are less commonly used. Their limitations, particularly with respect to material rheology and process parameters, make them less adaptable to a broad range of bioprinting applications. However, these technologies still hold potential in certain niche applications due to their ability to print with very low viscosity materials and their non-contact nature.

Among these, 2PP, though relatively new and with fewer

publications, offers unparalleled resolution. Capable of advancing towards single-cell precision, it represents a breakthrough in bioprinting, pushing the boundaries of what is achievable in terms of spatial control. However, due to the extremely small size of its constructs, 2PP is not yet applicable for large-scale tissue engineering but finds promise in specific applications such as in vitro models and microscale constructs that require fine spatiotemporal control.

In terms of materials, GelMA, Alginate, Collagen, and culture media are the most commonly used. Each material's specific properties make them more or less suitable for the different bioprinting techniques, with GelMA's versatility and tunability being particularly favored.

Resolution characterization has emerged as a critical area of interest, with growing attention being paid to how well different technologies can define fine features in printed structures. This review identifies the most common metrics used to evaluate resolution and underscores the challenge posed by the lack of standardization in evaluation methods. Each technology tends to adopt its own set of metrics, making it difficult to directly compare results across different studies. Establishing unified metrics and standardized protocols would not only simplify comparisons but also facilitate faster advancements in the field.

The field of 3D bioprinting is expanding rapidly, with substantial research focusing on both the technological and material fronts. Resolution, in particular, is gaining significant attention, and improving it is expected to be one of the key challenges for the future. As the demand for higher precision and more complex structures grows, researchers are moving beyond traditional approaches. Some studies are exploring the use of artificial intelligence to optimize bioprinting processes and predict outcomes more accurately [132,134], while others are modifying existing technologies to go beyond current technological limits [135]. Furthermore, there is increasing interest in delving deeper into the chemistry of polymers [136] and kinetics of photocrosslinking [137], aiming to optimize the polymerization process and lead to improvements in the resolution and fidelity of bioprinted structures.

Finally, recent works have demonstrated the potential of in-vivo bioprinting [87,138], a trend likely to expand with the advancement of new technologies like 2PP, which offers exceptional control and enables non-contact printing.

As these trends continue, 3D bioprinting is likely to evolve rapidly, with innovations in materials, techniques, and post-processing approaches likely to shape the next decade of advancements. The pursuit of higher resolution, combined with these innovations, will be critical in enabling more complex, functional tissues and pushing the boundaries of what is possible in regenerative medicine and beyond.

CRediT authorship contribution statement

Luca Guida: Writing – review & editing, Writing – original draft, Conceptualization. **Marco Cavallaro:** Writing – review & editing, Methodology, Conceptualization. **Marinella Levi:** Writing – review & editing, Methodology, Conceptualization.

Declaration of AI and AI-assisted technologies in the writing process

During the preparation of this work the authors used ChatGPT-3.5 in order to improve text clarity and readability. After using this tool, the authors reviewed and edited the content as needed and take full responsibility for the content of the publication.

Declaration of competing interest

The authors declare that they have no known competing financial interests or personal relationships that could have appeared to influence the work reported in this paper.

Appendix. A Reviewed literature

Table 3 lists eligible articles with most relevant information. Details about crosslinking agents, crosslinking strategies, printers, printing parameters and printed items are available in Supplementary Information.

Table 3
List of eligible articles. More details are available in supplementary information.

	Article	Technology	Material	Resolution
1	2024 Moon [50]	EBB	Silk fibroin 20 % + Iota-carrageenan 1–3%	A (Strand width) ≈ 1.5 Pr ~ 1
2	2024 Davern [53]	EBB	Gelma 5–15 % + Laponite 2 %	Pr = 0.95–1.05 W = 400–600 um
3	2024 Shyam [44]	EBB	Corn starch 10 % + Gelatin 3–10 %	Pr = 0.9–1.2
4	2023 Maciel [52]	EBB	Gelatin 6–8% + PVA 2–4% + Laponite 0.2–0.4 %	W ≈ 300 um
5	2023 Shehzad [110]	EBB	Alginate 1 % + Gelatin 2–8% + GelMA 2.5–10 %	A (Pore area) = 94 %
6	2023 Ng [51]	EBB	Gellan Gum 0.8 % + Pregelatinized starch 5 % + Glycerol 15 %	A (Strand width) = 1.09 A (Squares area) = 1.36
7	2023 Hibbert [58]	EBB	Alginate 4–6% + Pluronic F127 20–25 %	Pr ≈ 1 I = 0.99
8	2023 Boonlai [122]	EBB	Pluronic 14–20 % + Methylcellulose 4 %	Qualitative ("good printability")
9	2023 Tang [40]	EBB	GelMA 6–12 %	SPF (ID) = 70 μm SPF (Tw) = 4–15 um
10	2023 Moro [117]	EBB	Modified HA	W = 300 μm Pr = 0.95
11	2022 Bolivar-Monsalve [45]	EBB	GelMA 3 % + Alginate 3.5 %	SPF (ID) = 10–100 um
12	2022 Coskun [123]	EBB	Chitosan 2.3 % + Nano-hydroxyhapatite 0.23–0.92 %	Pr = 0.98
13	2022 Dutta [107]	EBB	Alginate 6 % + Gelatin 4 %	A (Pore area) = 1
14	2022 Navara [127]	EBB	Poly(N-isopropylacrylamide) 10–20 % + Poly(amidoamine) 7.5–15 %	Pr = 1.1 W ≈ 70 μm (32G)
15	2022 Anand [95]	EBB	Gelatin-hyaluronan dialdehyde 5 % + GelMA 5 %	Pr = 1.07
16	2022 Yao [115]	EBB	Norbornene-functionalized gelatin 2.8–6% + Poly(ethylene glycol-dithiol) 0.7–1.5 %	Pr = 0.82–0.87 W = 314 um
17	2022 Dorishetty [121]	EBB	Silk fibroin 15 % or Silk fibroin 15 % + rGO 0.05–0.13 %	A (Strand width) = 1.1 to 1.35

(continued on next page)

Table 3 (*continued*)

	Article	Technology	Material	Resolution
18	2022 Ravanbakhsh [96]	EBB	GelMa + DMSO	W = 250 um
19	2022 Kakarla [100]	EBB	Alginate 5 % + Boron Nitride nanotubes 0.05–1%	Pr = 1 A (Pore area) = 0.98
20	2021 Prendergast [56]	EBB	GelMA 3–10 % + Norbornene-functionalized HA nanofibers	W = 200 um
21	2021 Trucco [108]	EBB	Gelatin 5 % + Silk Fibroin 5 % or Gelatin 3 % + Alginate 7 %	W = 100 um
22	2021 Lin [103]	EBB	Collagen commercial ink (high conc.)	W = 190 um
23	2021 Bolívar-Monsalve [46]	EBB	GelMA 3–5% (Inner) GelMA 3 % + Alginate 1 % (Outer)	SPF: Lamellae thickness <50 um
24	2021 Aldana [111]	EBB	GelMA 8 % + Alginate 7 %	W = 740 μm A (Pore area) = 0.92
25	2021 Temirel [55]	EBB	Alginate 2 % + Cellulose nanocrystals 4 % or Alginate 4 % + Cellulose nanofibrils 1 %	W = 300 um
26	2020 Ngo [118]	EBB	Glycidyl methacrylate grafted-HA or Methactylic anhydride grafted-HA 0.5–4%	Pr ≈ 0.9 APr ≈ 0.8
27	2020 Sakai [57]	EBB	HA 1–1.5 % + Silk fibroin nanofibers 1 % or Gelatin 1 % + Silk fibroin nanofibers 1 %	W = 400 um
28	2020 Kang [42]	EBB	Collagen 1–6% + Alginate 1–5% (sacrificial)	C = 0.8 SPF (Tw) = 30 um
29	2020 Gantumur [54]	EBB	Alginate 0.5 % + Cellulose nanofibers 0.5–1.5 % + Glucose 4.4 %	W = 300 um
30	2020 Mendes [129]	EBB	Component 1: Platelet Lysate 16 % Component 2: Cellulose nanocrystals 2.88 % + Thrombin	W = 250 um
31	2019 Wang [39]	EBB	GelMA 5–10 % + Gelatin 3–8% (Outer) PVA 5 % (Inner, sacrificial)	SPF (ID) = 250 μm SPF (OD) = 650 um
32	2019 Kiyotake [48]	EBB	Pentenoate-functionalized hyaluronic acid 6–9% + Dithiothreitol (1:1 M ratio)	W = 450 um
33	2019 Zhuang [49]	EBB	GelMA 5–10 % + Gellan gum 0.1–0.5 %	W = 550 μm Qualitative ("Good printability")
34	2019 Sarker [47]	EBB	Peptide-conjugated alginate	Pr = 1 A (Angles) = 1.1
35	2018 Pi [41]	EBB	GelMA 7 % + Alginate 3 % + PEGOA 2 % + CaCl2 solution (sacrificial)	Two layers hollow tubes Inner shell: SPF (ID) = 600 μm SPF (Tw) = 60 μm Outer shell: SPF (OD) = 1 mm SPF (Tw) = 100 um
36	2018 Kang [43]	EBB	Collagen 5 % (Outer) Alginate 2–4 % (Inner)	W = 300 μm SPF = < 100 μm lobes
37	2018 Giuseppe [109]	EBB	Gelatin 8 % + Alginate 7 %	W = 310 μm A (Pore area) = 0.99
38	2018 Liu [38]	EBB	CaCl2 6 % (Inner) + Alginate 1 % (Outer) or GelMA 1–2 % (Inner) + Alginate 1 % (Outer)	SPF (ID) = 468 um
39	2017 England [128]	EBB	Fibrinogen 5 % + HA 0.4 %	W = 170 um
40	2023 You [76]	VP	GelMA 5 %	SPF = 50 um SPF (ID) = 250 um
41	2023 Shi [97]	VP	CollagenMA 1.5–2% or GelMA 5 %	**CollagenMA:** Ra = 38.66 μm **GelMA:** Ra = 16.32 um
42	2023 Duong [66]	VP	Norbornene-modified gelatin 2–6 %	Grid: A (Pore area) > 97 % Channels: SPF (ID) = 300–1200 um A (Perfusable length) > 80 %
43	2023 Dutta [116]	VP	Gelatin-Cellulose-PEGDA	Qualitative, ≈100 %
44	2023 Torras [65]	VP	GelMa 5 % PEGDA 3 %	I = 90 %
45	2023 Su [62]	VP	PEGDA 15 %	Channels: ID: 1 mm Ring:A (OD/ID ratio) ≈ 100 %
46	2023 Choi [67]	VP	GMA-grafted Silk fibroin + GMA-grafted Gelatin (20 % total dry fraction)	A (Channel side) ≈ 100 %
47	2023 Galarraga [119]	VP	Norbornene-modified HA 5 %	SPF = 500 μm pores
48	2023 Perez-Cortez [71]	VP	GelMA 7.5–10 %	100 μm pores: A = 0.95 1500 μm pores: A = 0.99
49	2022 Xie [63]	VP	GelMA 10 % + Cartilage acellular matrix 10 %	Pores: SPF (ID) = 200 μm Cylinders: SPF (OD) = 200 um
50	2022 Jeong [98]	VP	GelMa 10 %	SPF (ID) = 100 um
51	2022 Ma [64]	VP	GelMA 10 % or PEGDA 10 %	Hollow cylinders: SPF (Tw) = 10 μm Lines: W = 10 um
52	2022 Kumari [125]	VP	MA-κ-carrageenan 1–5 %	SPF = 800 μm features
53	2022 Lee [68]	VP	GMA-grafted fluorescent silk fibroin 20 %	Qualitative, good accuracy
54	2022 Viray [73]	VP	Poly(L-glutamic acid) conjugated with tyramine 5 %	W = 8 um
55	2022 Wu [70]	VP	CollagenMA 2 % + Procyanidin 2 %	**Grids:** SPF = 500 μm pores W = 200 um
56	2022 Chang [69]	VP	PEGDMA or PEGMA	SPF (ID) = 700 um
57	2022 Bhusal [75]	VP	PEGDA 20–40 % + GelMA 0–5 %	**Pores:** SPF = 15 μm side
58	2021 Grigoryan [74]	VP		SPF = 250 μm extrusions

(*continued on next page*)

Table 3 (*continued*)

	Article	Technology	Material	Resolution
59	2021 Li [112]	VP	PEGDA 40 %	SPF = 80 μm features
60	2021 Huh [113]	VP	4-PEGDA 8 %	SPF (ID) = 750 um
61	2021 Anandakrishnan [114]	VP	PEGDA 20 %	Qualitative, good printability of large scale structures
62	2021 Zhang [72]	VP	GelMa 5 %	SPF = 100 μm pores
63	2021 Kumar [60]	VP	GelMa 10 %	W = 250 um
64	2018 Lim [99]	VP	GelMA and PVAMA	**Channel:** SPF = 50 μm diameter
65	2018 Grix [61]	VP	PEG 7 % and GelMA 7 %	W = 191 um
66	2017 Sakai [59]	VP	Alginate derivative 1 %	**Grids:** W = 500 μm strands
67	2023 Ng [139]	Inkjet	Polyvinylpyrrolidone 0–2%	D_D = 0.345 nL
68	2022 Ng [104]	Inkjet	Culture medium	D_D = 0.345 nL
69	2020 Park [102]	Inkjet	Collagen 0.3 %	D_D = 70 μm CN = 0.1–1
70	2020 Masaeli [77]	Inkjet	Culture medium	D_D = 629 um
71	2020 Masaeli [78]	Inkjet	Culture medium	D_D = 300 pL CN = 93
72	2020 Dudman [81]	Inkjet	Culture medium	CN = 0-1
73	2019 Takagi [79]	Inkjet	Culture medium or Alginate 0.5 %	CN = 0-2
74	2017 Park [80]	Inkjet	Culture medium	CN = 2
75	2017 Hewes [82]	Inkjet	Alginate 0.7 %	SPF(ID) = 300 μm D_D = 40 μm CN = 0.67
76	2017 Compaan [83]	Inkjet	Silk fibroin 4 % + Alginate 0.5 %	SPF(Tw) = 400 um
77	2023 Shakil [85]	LIFT	Collagen I 0.075–0.1 % + Glycerol	D_D = 100 um
78	2022 Karakaidos [105]	LIFT	Culture medium	D_D = 250 μm CN = 170
79	2021 Kryou [106]	LIFT	Culture medium	D_D = 230 um
80	2020 Marquez [101]	LIFT	Alginate 1.5–2% or Methylcellulose 0.3–1.5 %	D_D = 80 um
81	2017 Xiong [86]	LIFT	Alginate 1–4%	D_D = 100 um
82	2017 Koch [84]	LIFT	Alginate 4 %: EDTA blood plasma 1:1	D_D = 100 um
83	2023 Rizzo [120]	2PP	Hyaluronic acid maleimide 0.5 %	SPF = 1 μm (Both positive and negative features)
84	2023 Taale [91]	2PP	Gelatin-based commercial ink	SPF = 260 μm Hollow sphere SPF(ID) = 20 μm (pores on sphere surface) SPF(Tw) = 50 μm (Sphere wall)
85	2022 Valente [90]	2PP	Silk Fibroin 4 %	Qualitative
86	2020 Dobos [89]	2PP	Norbornene-modified gelatin + Thiol-modified gelatin 3.75 + 3.75 %	SFF = 1 SPF(ID) = 30 um
87	2020 Tytgat [88]	2PP	Norbornene and thiol-functionalized collagen (1:1 ratio) 7.5–10 % or Methacrylamide-functionalized collagen 7.5–10 %	SPF = 20 μm features
88	2020 Urciuolo [87]	2PP	HCC-modified gelatin	**Lines:** W = 1.9 um SPF = 0.5 μm Distance between lines

Appendix A. Supplementary data

Supplementary data to this article can be found online at https://doi.org/10.1016/j.bprint.2024.e00376.

Data availability

Data will be made available on request.

References

[1] R. Klebe, Cytoscribing: a method for micropositioning cells and the construction of two- and three-dimensional synthetic tissues, Exp. Cell Res. 179 (1988) 362–373, https://doi.org/10.1016/0014-4827(88)90275-3.

[2] I.T. Ozbolat, Yin Yu, Bioprinting toward organ fabrication: challenges and future trends, IEEE Trans. Biomed. Eng. 60 (2013) 691–699, https://doi.org/10.1109/TBME.2013.2243912.

[3] M. Hospodiuk, M. Dey, D. Sosnoski, I.T. Ozbolat, The bioink: a comprehensive review on bioprintable materials, Biotechnol. Adv. 35 (2017) 217–239, https://doi.org/10.1016/j.biotechadv.2016.12.006.

[4] J. Groll, J.A. Burdick, D.-W. Cho, B. Derby, M. Gelinsky, S.C. Heilshorn, T. Jüngst, J. Malda, V.A. Mironov, K. Nakayama, A. Ovsianikov, W. Sun, S. Takeuchi, J. J. Yoo, T.B.F. Woodfield, A definition of bioinks and their distinction from biomaterial inks, Biofabrication 11 (2018) 013001, https://doi.org/10.1088/1758-5090/aaec52.

[5] C. Mandrycky, Z. Wang, K. Kim, D.-H. Kim, 3D bioprinting for engineering complex tissues, Biotechnol. Adv. 34 (2016) 422–434, https://doi.org/10.1016/j.biotechadv.2015.12.011.

[6] D.W. Hutmacher, M. Sittinger, M. V Risbud, Scaffold-based tissue engineering: rationale for computer-aided design and solid free-form fabrication systems, Trends Biotechnol. 22 (2004) 354–362, https://doi.org/10.1016/j.tibtech.2004.05.005.

[7] T.H. Ang, F.S.A. Sultana, D.W. Hutmacher, Y.S. Wong, J.Y.H. Fuh, X.M. Mo, H. T. Loh, E. Burdet, S.H. Teoh, Fabrication of 3D chitosan–hydroxyapatite scaffolds using a robotic dispensing system, Mater. Sci. Eng. C 20 (2002) 35–42, https://doi.org/10.1016/S0928-4931(02)00010-3.

[8] T. Xu, J. Jin, C. Gregory, J.J. Hickman, T. Boland, Inkjet printing of viable mammalian cells, Biomaterials 26 (2005) 93–99, https://doi.org/10.1016/j.biomaterials.2004.04.011.

[9] M. Gruene, A. Deiwick, L. Koch, S. Schlie, C. Unger, N. Hofmann, I. Bernemann, B. Glasmacher, B. Chichkov, Laser printing of stem cells for biofabrication of scaffold-free autologous grafts, Tissue Eng. C Methods 17 (2011) 79–87, https://doi.org/10.1089/ten.tec.2010.0359.

[10] M.N. Cooke, J.P. Fisher, D. Dean, C. Rimnac, A.G. Mikos, Use of stereolithography to manufacture critical-sized 3D biodegradable scaffolds for bone ingrowth, J. Biomed. Mater. Res. B Appl. Biomater. 64B (2003) 65–69, https://doi.org/10.1002/jbm.b.10485.

[11] P. Timashev, D. Kuznetsova, A. Koroleva, N. Prodanets, A. Deiwick, Y. Piskun, K. Bardakova, N. Dzhoyashvili, S. Kostjuk, E. Zagaynova, Y. Rochev, B. Chichkov, V. Bagratashvili, Novel biodegradable star-shaped polylactide scaffolds for bone regeneration fabricated by two-photon polymerization, Nanomedicine 11 (2016) 1041–1053, https://doi.org/10.2217/nnm-2015-0022.

[12] S. Boularaoui, G. Al Hussein, K.A. Khan, N. Christoforou, C. Stefanini, An overview of extrusion-based bioprinting with a focus on induced shear stress and its effect on cell viability, Bioprinting 20 (2020) e00093, https://doi.org/10.1016/j.bprint.2020.e00093.

[13] L. Moroni, J.A. Burdick, C. Highley, S.J. Lee, Y. Morimoto, S. Takeuchi, J.J. Yoo, Biofabrication strategies for 3D in vitro models and regenerative medicine, Nat. Rev. Mater. 3 (2018) 21–37, https://doi.org/10.1038/s41578-018-0006-y.

[14] S. Derakhshanfar, R. Mbeleck, K. Xu, X. Zhang, W. Zhong, M. Xing, 3D bioprinting for biomedical devices and tissue engineering: a review of recent trends and advances, Bioact. Mater. 3 (2018) 144–156, https://doi.org/10.1016/j.bioactmat.2017.11.008.

[15] J. Malda, J. Visser, F.P. Melchels, T. Jüngst, W.E. Hennink, W.J.A. Dhert, J. Groll, D.W. Hutmacher, 25th anniversary article: engineering hydrogels for biofabrication, Adv. Mater. 25 (2013) 5011–5028, https://doi.org/10.1002/adma.201302042.

[16] T. Xu, W. Zhao, J.-M. Zhu, M.Z. Albanna, J.J. Yoo, A. Atala, Complex heterogeneous tissue constructs containing multiple cell types prepared by inkjet printing technology, Biomaterials 34 (2013) 130–139, https://doi.org/10.1016/j.biomaterials.2012.09.035.

[17] H. Xu, J. Casillas, C. Xu, Effects of printing conditions on cell distribution within microspheres during inkjet-based bioprinting, AIP Adv. 9 (2019), https://doi.org/10.1063/1.5116371.

[18] H. Xu, D.M. Martinez Salazar, C. Xu, Investigation of cell concentration change and cell aggregation due to cell sedimentation during inkjet-based bioprinting of cell-laden bioink, Machines 10 (2022) 315, https://doi.org/10.3390/machines10050315.

[19] H. Xu, D.M. Martinez Salazar, M. Shahriar, C. Xu, Investigation and characterization of cell aggregation during and after inkjet-based bioprinting of cell-laden bioink, J. Manuf. Sci. Eng. 144 (2022), https://doi.org/10.1115/1.4054640.

[20] Z. Kanaki, C. Chandrinou, I.-M. Orfanou, C. Kryou, J. Ziesmer, G.A. Sotiriou, A. Klinakis, C. Tamvakopoulos, I. Zergioti, Laser-induced forward transfer printing on microneedles for transdermal delivery of gemcitabine, Int J Bioprint 8 (2022) 554, https://doi.org/10.18063/ijb.v8i2.554.

[21] J. Chang, X. Sun, Laser-induced forward transfer based laser bioprinting in biomedical applications, Front. Bioeng. Biotechnol. 11 (2023), https://doi.org/10.3389/fbioe.2023.1255782.

[22] M. Lee, R. Rizzo, F. Surman, M. Zenobi-Wong, Guiding lights: tissue bioprinting using photoactivated materials, Chem. Rev. 120 (2020) 10950–11027, https://doi.org/10.1021/acs.chemrev.0c00077.

[23] N.A. Chartrain, C.B. Williams, A.R. Whittington, A review on fabricating tissue scaffolds using vat photopolymerization, Acta Biomater. 74 (2018) 90–111, https://doi.org/10.1016/j.actbio.2018.05.010.

[24] I. Gibson, D. Rosen, B. Stucker, M. Khorasani, Vat photopolymerization, in: Additive Manufacturing Technologies, Springer International Publishing, Cham, 2021, pp. 77–124, https://doi.org/10.1007/978-3-030-56127-7_4.

[25] W.L. Ng, J.M. Lee, M. Zhou, Y.-W. Chen, K.-X.A. Lee, W.Y. Yeong, Y.-F. Shen, Vat polymerization-based bioprinting—process, materials, applications and regulatory challenges, Biofabrication 12 (2020) 022001, https://doi.org/10.1088/1758-5090/ab6034.

[26] K. Arcaute, B. Mann, R. Wicker, Stereolithography of spatially controlled multi-material bioactive poly(ethylene glycol) scaffolds, Acta Biomater. 6 (2010) 1047–1054, https://doi.org/10.1016/j.actbio.2009.08.017.

[27] M.A. Chliara, S. Elezoglou, I. Zergioti, Bioprinting on organ-on-chip: development and applications, Biosensors 12 (2022) 1135, https://doi.org/10.3390/bios12121135.

[28] X. Zhou, Y. Hou, J. Lin, A review on the processing accuracy of two-photon polymerization, AIP Adv. 5 (2015), https://doi.org/10.1063/1.4916886.

[29] X. Huang, Y. Zhang, M. Shi, L.-P. Zhang, Y. Zhang, Y. Zhao, A highly biocompatible bio-ink for 3D hydrogel scaffolds fabrication in the presence of living cells by two-photon polymerization, Eur. Polym. J. 153 (2021) 110505, https://doi.org/10.1016/j.eurpolymj.2021.110505.

[30] V.F. Paz, M. Emons, K. Obata, A. Ovsianikov, S. Peterhänsel, K. Frenner, C. Reinhardt, B. Chichkov, U. Morgner, W. Osten, Development of functional sub-100 nm structures with 3D two-photon polymerization technique and optical methods for characterization, J. Laser Appl. 24 (2012), https://doi.org/10.2351/1.4712151.

[31] M.W. Tibbitt, J.A. Shadish, C.A. DeForest, Photopolymers for multiphoton lithography in biomaterials and hydrogels, in: Multiphoton Lithography, Wiley, 2016, pp. 183–220, https://doi.org/10.1002/9783527682676.ch8.

[32] M.C. Echave, P. Sánchez, J.L. Pedraz, G. Orive, Progress of gelatin-based 3D approaches for bone regeneration, J. Drug Deliv. Sci. Technol. 42 (2017) 63–74, https://doi.org/10.1016/j.jddst.2017.04.012.

[33] S.Y. Sonaye, E.G. Ertugral, C.R. Kothapalli, P. Sikder, Extrusion 3D (Bio)Printing of alginate-gelatin-based composite scaffolds for skeletal muscle tissue engineering, Materials 15 (2022) 7945, https://doi.org/10.3390/ma15227945.

[34] O. Messaoudi, C. Henrionnet, K. Bourge, D. Loeuille, P. Gillet, A. Pinzano, Stem cells and extrusion 3D printing for hyaline cartilage engineering, Cells 10 (2020) 2, https://doi.org/10.3390/cells10010002.

[35] R. Liang, Y. Gu, Y. Wu, V. Bunpetch, S. Zhang, Lithography-based 3D bioprinting and bioinks for bone repair and regeneration, ACS Biomater. Sci. Eng. 7 (2021) 806–816, https://doi.org/10.1021/acsbiomaterials.9b01818.

[36] T. Zandrini, S. Florczak, R. Levato, A. Ovsianikov, Breaking the resolution limits of 3D bioprinting: future opportunities and present challenges, Trends Biotechnol. 41 (2023) 604–614, https://doi.org/10.1016/j.tibtech.2022.10.009.

[37] C.-F. He, T.-H. Qiao, G.-H. Wang, Y. Sun, Y. He, High-resolution projection-based 3D bioprinting, Nature Reviews Bioengineering (2024), https://doi.org/10.1038/s44222-024-00218-w.

[38] W. Liu, Z. Zhong, N. Hu, Y. Zhou, L. Maggio, A.K. Miri, A. Fragasso, X. Jin, A. Khademhosseini, Y.S. Zhang, Coaxial extrusion bioprinting of 3D microfibrous constructs with cell-favorable gelatin methacryloyl microenvironments, Biofabrication 10 (2018) 024102, https://doi.org/10.1088/1758-5090/aa9d44.

[39] Y. Wang, R.K. Kankala, K. Zhu, S.-B. Wang, Y.S. Zhang, A.-Z. Chen, Coaxial extrusion of tubular tissue constructs using a gelatin/GelMA blend bioink, ACS Biomater. Sci. Eng. 5 (2019) 5514–5524, https://doi.org/10.1021/acsbiomaterials.9b00926.

[40] G. Tang, Z. Luo, L. Lian, J. Guo, S. Maharjan, C.E. Garciamendez-Mijares, M. Wang, W. Li, Z. Zhang, D. Wang, M. Xie, H. Ravanbakhsh, C. Zhou, X. Kuang, Y. Hou, X. Yu, Y.S. Zhang, Liquid-embedded (bio)printing of alginate-free, standalone, ultrafine, and ultrathin-walled cannular structures, Proc. Natl. Acad. Sci. USA 120 (2023), https://doi.org/10.1073/pnas.2206762120.

[41] Q. Pi, S. Maharjan, X. Yan, X. Liu, B. Singh, A.M. van Genderen, F. Robledo-Padilla, R. Parra-Saldivar, N. Hu, W. Jia, C. Xu, J. Kang, S. Hassan, H. Cheng, X. Hou, A. Khademhosseini, Y.S. Zhang, Digitally tunable microfluidic bioprinting of multilayered cannular tissues, Adv. Mater. 30 (2018), https://doi.org/10.1002/adma.201706913.

[42] D. Kang, G. Hong, S. An, I. Jang, W. Yun, J. Shim, S. Jin, Bioprinting of multiscaled hepatic lobules within a highly vascularized construct, Small 16 (2020), https://doi.org/10.1002/smll.201905505.

[43] D. Kang, G. Ahn, D. Kim, H.-W. Kang, S. Yun, W.-S. Yun, J.-H. Shim, S. Jin, Pre-set extrusion bioprinting for multiscale heterogeneous tissue structure fabrication, Biofabrication 10 (2018) 035008, https://doi.org/10.1088/1758-5090/aac70b.

[44] R. Shyam, A. Palaniappan, Development and optimization of starch-based biomaterial inks and the effect of infill patterns on the mechanical, physicochemical, and biological properties of 3D printed scaffolds for tissue engineering, Int. J. Biol. Macromol. 258 (2024) 128986, https://doi.org/10.1016/j.ijbiomac.2023.128986.

[45] E.J. Bolívar-Monsalve, C.F. Ceballos-González, C. Chávez-Madero, B.G. de la Cruz-Rivas, S. Velásquez Marín, S. Mora-Godínez, L.M. Reyes-Cortés, A. Khademhosseini, P.S. Weiss, M. Samandari, A. Tamayol, M.M. Alvarez, G. Trujillo-de Santiago, One-step bioprinting of multi-channel hydrogel filaments using chaotic advection: fabrication of pre-vascularized muscle-like tissues, Adv. Healthcare Mater. 11 (2022), https://doi.org/10.1002/adhm.202200448.

[46] E.J. Bolívar-Monsalve, C.F. Ceballos-González, K.I. Borrayo-Montaño, D. A. Quevedo-Moreno, J.F. Yee-de León, A. Khademhosseini, P.S. Weiss, M. M. Alvarez, G. Trujillo-de Santiago, Continuous chaotic bioprinting of skeletal muscle-like constructs, Bioprinting 21 (2021) e00125, https://doi.org/10.1016/j.bprint.2020.e00125.

[47] M.D. Sarker, S. Naghieh, A.D. McInnes, L. Ning, D.J. Schreyer, X. Chen, Bio-fabrication of peptide-modified alginate scaffolds: printability, mechanical stability and neurite outgrowth assessments, Bioprinting 14 (2019) e00045, https://doi.org/10.1016/j.bprint.2019.e00045.

[48] E.A. Kiyotake, A.W. Douglas, E.E. Thomas, S.L. Nimmo, M.S. Detamore, Development and quantitative characterization of the precursor rheology of hyaluronic acid hydrogels for bioprinting, Acta Biomater. 95 (2019) 176–187, https://doi.org/10.1016/j.actbio.2019.01.041.

[49] P. Zhuang, W.L. Ng, J. An, C.K. Chua, L.P. Tan, Layer-by-layer ultraviolet assisted extrusion-based (UAE) bioprinting of hydrogel constructs with high aspect ratio for soft tissue engineering applications, PLoS One 14 (2019) e0216776, https://doi.org/10.1371/journal.pone.0216776.

[50] S.H. Moon, T.Y. Park, H.J. Cha, Y.J. Yang, Photo-/thermo-responsive bioink for improved printability in extrusion-based bioprinting, Mater Today Bio 25 (2024) 100973, https://doi.org/10.1016/j.mtbio.2024.100973.

[51] J.Y. Ng, P. Yu, D.M. Murali, Y.-S. Liu, R. Gokhale, P.L.R. Ee, The influence of pregelatinized starch on the rheology of a gellan gum-collagen IPN hydrogel for 3D bioprinting, Chem. Eng. Res. Des. 192 (2023) 477–486, https://doi.org/10.1016/j.cherd.2023.02.042.

[52] B.R. Maciel, A. Grimm, C. Oelschlaeger, U. Schepers, N. Willenbacher, Targeted micro-heterogeneity in bioinks allows for 3D printing of complex constructs with improved resolution and cell viability, Biofabrication 15 (2023) 045013, https://doi.org/10.1088/1758-5090/acee22.

[53] J.W. Davern, L. Hipwood, L.J. Bray, C. Meinert, T.J. Klein, Addition of Laponite to gelatin methacryloyl bioinks improves the rheological properties and printability to create mechanically tailorable cell culture matrices, APL Bioeng. 8 (2024), https://doi.org/10.1063/5.0166206.

[54] E. Gantumur, M. Nakahata, M. Kojima, S. Sakai, Extrusion-based bioprinting through glucose-mediated enzymatic hydrogelation, Int J Bioprint 6 (2020) 43–52, https://doi.org/10.18063/ijb.v6i1.250.

[55] M. Temirel, C. Hawxhurst, S. Tasoglu, Shape fidelity of 3D-bioprinted biodegradable patches, Micromachines 12 (2021) 195, https://doi.org/10.3390/mi12020195.

[56] M.E. Prendergast, M.D. Davidson, J.A. Burdick, A biofabrication method to align cells within bioprinted photocrosslinkable and cell-degradable hydrogel constructs via embedded fibers, Biofabrication 13 (2021) 044108, https://doi.org/10.1088/1758-5090/ac25cc.

[57] S. Sakai, A. Yoshii, S. Sakurai, K. Horii, O. Nagasuna, Silk fibroin nanofibers: a promising ink additive for extrusion three-dimensional bioprinting, Mater Today Bio 8 (2020) 100078, https://doi.org/10.1016/j.mtbio.2020.100078.

[58] M. Hibbert, J.M. Viljoen, L.H. du Plessis, Print parameter optimisation for a Pluronic F-127 and alginate hybrid hydrogel, Bioprinting 30 (2023) e00257, https://doi.org/10.1016/j.bprint.2022.e00257.

[59] S. Sakai, H. Kamei, T. Mori, T. Hotta, H. Ohi, M. Nakahata, M. Taya, Visible light-induced hydrogelation of an alginate derivative and application to stereolithographic bioprinting using a visible light projector and acid red, Biomacromolecules 19 (2018) 672–679, https://doi.org/10.1021/acs.biomac.7b01827.

[60] H. Kumar, K. Sakthivel, M.G.A. Mohamed, E. Boras, S.R. Shin, K. Kim, Designing gelatin methacryloyl (GelMA)-Based bioinks for visible light stereolithographic 3D biofabrication, Macromol. Biosci. 21 (2021), https://doi.org/10.1002/mabi.202000317.

[61] T. Grix, A. Ruppelt, A. Thomas, A.-K. Amler, B. Noichl, R. Lauster, L. Kloke, Bioprinting perfusion-enabled liver Equivalents for advanced organ-on-a-chip applications, Genes 9 (2018) 176, https://doi.org/10.3390/genes9040176.

[62] H. Su, B. Lu, M. Li, X. Yang, M. Qin, Y. Wu, Development of digital light processing-based multi-material bioprinting for fabrication of heterogeneous tissue constructs, Biomater. Sci. 11 (2023) 6663–6673, https://doi.org/10.1039/D3BM01054F.

[63] X. Xie, S. Wu, S. Mou, N. Guo, Z. Wang, J. Sun, Microtissue-based bioink as a chondrocyte microshelter for DLP bioprinting, Adv. Healthcare Mater. 11 (2022), https://doi.org/10.1002/adhm.202201877.

[64] Y. Ma, W. Wei, L. Gong, C. Li, Y. Hong, X. Wang, R. Liang, Q. Shao, Q. Liang, W. Huang, M.J. Shipston, H. Ouyang, Biomacromolecule-based agent for high-precision light-based 3D hydrogel bioprinting, Cell Rep Phys Sci 3 (2022) 100985, https://doi.org/10.1016/j.xcrp.2022.100985.

[65] N. Torras, J. Zabalo, E. Abril, A. Carré, M. García-Díaz, E. Martínez, A bioprinted 3D gut model with crypt-villus structures to mimic the intestinal epithelial-stromal microenvironment, Biomater. Adv. 153 (2023) 213534, https://doi.org/10.1016/j.bioadv.2023.213534.

[66] V.T. Duong, C. Lin, Digital light processing 3D bioprinting of gelatin-norbornene hydrogel for enhanced vascularization, Macromol. Biosci. 23 (2023), https://doi.org/10.1002/mabi.202300213.

[67] K.Y. Choi, O. Ajiteru, H. Hong, Y.J. Suh, M.T. Sultan, H. Lee, J.S. Lee, Y.J. Lee, O. J. Lee, S.H. Kim, C.H. Park, A digital light processing 3D-printed artificial skin model and full-thickness wound models using silk fibroin bioink, Acta Biomater. 164 (2023) 159–174, https://doi.org/10.1016/j.actbio.2023.04.034.

[68] Y.J. Lee, J.S. Lee, O. Ajiteru, O.J. Lee, J.S. Lee, H. Lee, S.W. Kim, J.W. Park, K. Y. Kim, K.Y. Choi, H. Hong, T. Sultan, S.H. Kim, C.H. Park, Biocompatible fluorescent silk fibroin bioink for digital light processing 3D printing, Int. J. Biol. Macromol. 213 (2022) 317–327, https://doi.org/10.1016/j.ijbiomac.2022.05.123.

[69] S.-Y. Chang, T. Ching, M. Hashimoto, Bioprinting using PEGDMA-based hydrogel on DLP printer, Mater. Today Proc. 70 (2022) 179–183, https://doi.org/10.1016/j.matpr.2022.09.017.

[70] Z. Wu, J. Liu, J. Lin, L. Lu, J. Tian, L. Li, C. Zhou, Novel digital light processing printing strategy using a collagen-based bioink with prospective cross-linker procyanidins, Biomacromolecules 23 (2022) 240–252, https://doi.org/10.1021/acs.biomac.1c01244.

[71] J. Pérez-Cortez, V. Sánchez-Rodríguez, S. Gallegos-Martínez, C. Chuck-Hernández, C. Rodriguez, M. Álvarez, G. Trujillo-de Santiago, E. Vázquez-Lepe, J. Martínez-López, Low-cost light-based GelMA 3D bioprinting via retrofitting: manufacturability test and cell culture assessment, Micromachines 14 (2022) 55, https://doi.org/10.3390/mi14010055.

[72] P. Zhang, H. Wang, P. Wang, Y. Zheng, L. Liu, J. Hu, Y. Liu, Q. Gao, Y. He, Lightweight 3D bioprinting with point by point photocuring, Bioact. Mater. 6 (2021) 1402–1412, https://doi.org/10.1016/j.bioactmat.2020.10.023.

[73] C.M. Viray, B. van Magill, H. Zreiqat, Y. Ramaswamy, Stereolithographic visible-light printing of poly(<scp>l</scp> -glutamic acid) hydrogel scaffolds, ACS Biomater. Sci. Eng. 8 (2022) 1115–1131, https://doi.org/10.1021/acsbiomaterials.1c01519.

[74] B. Grigoryan, D.W. Sazer, A. Avila, J.L. Albritton, A. Padhye, A.H. Ta, P. T. Greenfield, D.L. Gibbons, J.S. Miller, Development, characterization, and applications of multi-material stereolithography bioprinting, Sci. Rep. 11 (2021) 3171, https://doi.org/10.1038/s41598-021-82102-w.

[75] A. Bhusal, E. Dogan, H.-A. Nguyen, O. Labutina, D. Nieto, A. Khademhosseini, A. K. Miri, Multi-material digital light processing bioprinting of hydrogel-based microfluidic chips, Biofabrication 14 (2022) 014103, https://doi.org/10.1088/1758-5090/ac2d78.

[76] S. You, Y. Xiang, H.H. Hwang, D.B. Berry, W. Kiratitanaporn, J. Guan, E. Yao, M. Tang, Z. Zhong, X. Ma, D. Wangpraseurt, Y. Sun, T. Lu, S. Chen, High cell density and high-resolution 3D bioprinting for fabricating vascularized tissues, Sci. Adv. 9 (2023), https://doi.org/10.1126/sciadv.ade7923.

[77] E. Masaeli, C. Marquette, Direct-write bioprinting approach to construct multilayer cellular tissues, Front. Bioeng. Biotechnol. 7 (2020), https://doi.org/10.3389/fbioe.2019.00478.

[78] E. Masaeli, V. Forster, S. Picaud, F. Karamali, M.H. Nasr-Esfahani, C. Marquette, Tissue engineering of retina through high resolution 3-dimensional inkjet bioprinting, Biofabrication 12 (2020) 025006, https://doi.org/10.1088/1758-5090/ab4a20.

[79] D. Takagi, W. Lin, T. Matsumoto, H. Yaginuma, N. Hemmi, S. Hatada, M. Seo, High-precision three-dimensional inkjet technology for live cell bioprinting, Int J Bioprint 5 (2019) 27–38, https://doi.org/10.18063/ijb.v5i2.208.

[80] J.A. Park, S. Yoon, J. Kwon, H. Now, Y.K. Kim, W.-J. Kim, J.-Y. Yoo, S. Jung, Freeform micropatterning of living cells into cell culture medium using direct inkjet printing, Sci. Rep. 7 (2017) 14610, https://doi.org/10.1038/s41598-017-14726-w.

[81] J.P.R. Dudman, A.M. Ferreira, P. Gentile, X. Wang, R.D.C. Ribeiro, M. Benning, K. W. Dalgarno, Reliable inkjet printing of chondrocytes and MSCs using reservoir agitation, Biofabrication 12 (2020) 045024, https://doi.org/10.1088/1758-5090/aba2f8.

[82] S. Hewes, A.D. Wong, P.C. Searson, Bioprinting microvessels using an inkjet printer, Bioprinting 7 (2017) 14–18, https://doi.org/10.1016/j.bprint.2017.05.002.

[83] A.M. Compaan, K. Christensen, Y. Huang, Inkjet bioprinting of 3D silk fibroin cellular constructs using sacrificial alginate, ACS Biomater. Sci. Eng. 3 (2017) 1519–1526, https://doi.org/10.1021/acsbiomaterials.6b00432.

[84] L. Koch, O. Brandt, A. Deiwick, B. Chichkov, Laser-assisted bioprinting at different wavelengths and pulse durations with a metal dynamic release layer: a parametric study, Int J Bioprint 3 (2017) 42–53, https://doi.org/10.18063/IJB.2017.01.001.

[85] M. Shakil Arman, B. Xu, A. Tsin, J. Li, Laser-induced forward transfer (LIFT) based bioprinting of the collagen I with retina photoreceptor cells, Manuf Lett 35 (2023) 477–484, https://doi.org/10.1016/j.mfglet.2023.07.005.

[86] R. Xiong, Z. Zhang, W. Chai, D.B. Chrisey, Y. Huang, Study of gelatin as an effective energy absorbing layer for laser bioprinting, Biofabrication 9 (2017) 024103, https://doi.org/10.1088/1758-5090/aa74f2.

[87] A. Urciuolo, I. Poli, L. Brandolino, P. Raffa, V. Scattolini, C. Laterza, G.G. Giobbe, E. Zambaiti, G. Selmin, M. Magnussen, L. Brigo, P. De Coppi, S. Salmaso, M. Giomo, N. Elvassore, Intravital three-dimensional bioprinting, Nat. Biomed. Eng. 4 (2020) 901–915, https://doi.org/10.1038/s41551-020-0568-z.

[88] L. Tytgat, A. Dobos, M. Markovic, L. Van Damme, J. Van Hoorick, F. Bray, H. Thienpont, H. Ottevaere, P. Dubruel, A. Ovsianikov, S. Van Vlierberghe, High-resolution 3D bioprinting of photo-cross-linkable recombinant collagen to serve tissue engineering applications, Biomacromolecules 21 (2020) 3997–4007, https://doi.org/10.1021/acs.biomac.0c00386.

[89] A. Dobos, F. Gantner, M. Markovic, J. Van Hoorick, L. Tytgat, S. Van Vlierberghe, A. Ovsianikov, On-chip high-definition bioprinting of microvascular structures, Biofabrication 13 (2021) 015016, https://doi.org/10.1088/1758-5090/abb063.

[90] F. Valente, M.S. Hepburn, J. Chen, A.A. Aldana, B.J. Allardyce, S. Shafei, B. J. Doyle, B.F. Kennedy, R.J. Dilley, Bioprinting silk fibroin using two-photon lithography enables control over the physico-chemical material properties and cellular response, Bioprinting 25 (2022) e00183, https://doi.org/10.1016/j.bprint.2021.e00183.

[91] M. Taale, B. Schamberger, F. Taheri, Y. Antonelli, A. Leal-Egaña, C. Selhuber-Unkel, In situ fabrication of constraints for multicellular micro-spheroids using two-photon lithography, Adv. Funct. Mater. (2023), https://doi.org/10.1002/adfm.202302356.

[92] T. Xu, S. Petridou, E.H. Lee, E.A. Roth, N.R. Vyavahare, J.J. Hickman, T. Boland, Construction of high-density bacterial colony arrays and patterns by the ink-jet method, Biotechnol. Bioeng. 85 (2004) 29–33, https://doi.org/10.1002/bit.10768.

[93] A. Urciuolo, G.G. Giobbe, Y. Dong, F. Michielin, L. Brandolino, M. Magnussen, O. Gagliano, G. Selmin, V. Scattolini, P. Raffa, P. Caccin, S. Shibuya, D. Scaglioni, X. Wang, J. Qu, M. Nikolic, M. Montagner, G.L. Galea, H. Clevers, M. Giomo, P. De Coppi, N. Elvassore, Hydrogel-in-hydrogel live bioprinting for guidance and control of organoids and organotypic cultures, Nat. Commun. 14 (2023) 3128, https://doi.org/10.1038/s41467-023-37953-4.

[94] N.F. Hasselmann, W. Horn, Attachment of microstructures to single bacteria by two-photon patterning of a protein based hydrogel, Biomed Phys Eng Express 4 (2018) 035004, https://doi.org/10.1088/2057-1976/aaafb7.

[95] R. Anand, M. Salar Amoli, A.-S. Huysecom, P.A. Amorim, H. Agten, L. Geris, V. Bloemen, A tunable gelatin-hyaluronan dialdehyde/methacryloyl gelatin interpenetrating polymer network hydrogel for additive tissue manufacturing, Biomed. Mater. 17 (2022) 045027, https://doi.org/10.1088/1748-605X/ac78b8.

[96] H. Ravanbakhsh, Z. Luo, X. Zhang, S. Maharjan, H.S. Mirkarimi, G. Tang, C. Chávez-Madero, L. Mongeau, Y.S. Zhang, Freeform cell-laden cryobioprinting for shelf-ready tissue fabrication and storage, Matter 5 (2022) 573–593, https://doi.org/10.1016/j.matt.2021.11.020.

[97] H. Shi, Y. Li, K. Xu, J. Yin, Advantages of photo-curable collagen-based cell-laden bioinks compared to methacrylated gelatin (GelMA) in digital light processing (DLP) and extrusion bioprinting, Mater Today Bio 23 (2023) 100799, https://doi.org/10.1016/j.mtbio.2023.100799.

[98] D. Jeong, J.W. Seo, H. Lee, W.K. Jung, Y.H. Park, H. Bae, Efficient myogenic/adipogenic transdifferentiation of bovine fibroblasts in a 3D bioprinting system for steak-type cultured meat production, Adv. Sci. 9 (2022), https://doi.org/10.1002/advs.202202877.

[99] K.S. Lim, R. Levato, P.F. Costa, M.D. Castilho, C.R. Alcala-Orozco, K.M.A. van Dorenmalen, F.P.W. Melchels, D. Gawlitta, G.J. Hooper, J. Malda, T.B. F. Woodfield, Bio-resin for high resolution lithography-based biofabrication of complex cell-laden constructs, Biofabrication 10 (2018) 034101, https://doi.org/10.1088/1758-5090/aac00c.

[100] A.B. Kakarla, I. Kong, C. Kong, H. Irving, Extrusion-based bioprinted boron nitride nanotubes reinforced alginate scaffolds: mechanical, printability and cell viability evaluation, Polymers 14 (2022) 486, https://doi.org/10.3390/polym14030486.

[101] A. Marquez, M. Gómez-Fontela, S. Lauzurica, R. Candorcio-Simón, D. Munoz-Martin, M. Morales, M. Ubago, C. Toledo, P. Lauzurica, C. Molpeceres, Fluorescence enhanced BA-LIFT for single cell detection and isolation, Biofabrication 12 (2020) 025019, https://doi.org/10.1088/1758-5090/ab6138.

[102] J.A. Park, H. Lee, S. Park, S. Jung, Self-organization of fibroblast-laden 3D collagen microstructures from inkjet-printed cell patterns, Adv Biosyst 4 (2020), https://doi.org/10.1002/adbi.201900280.

[103] H.-H. Lin, P.-H.G. Chao, W.-C. Tai, P.-C. Chang, 3D-Printed collagen-based waveform microfibrous scaffold for periodontal ligament reconstruction, Int. J. Mol. Sci. 22 (2021) 7725, https://doi.org/10.3390/ijms22147725.

[104] W.L. Ng, H. Xi, V. Shkolnikov, G.L. Goh, R. Suntornnond, W.Y. Yeong, Controlling droplet impact velocity and droplet volume: key factors to achieving high cell viability in sub-nanoliter droplet-based bioprinting, Int J Bioprint 8 (2021) 424, https://doi.org/10.18063/ijb.v8i1.424.
[105] P. Karakaidos, C. Kryou, N. Simigdala, A. Klinakis, I. Zergioti, Laser bioprinting of cells using UV and visible wavelengths: a comparative dna damage study, Bioengineering 9 (2022) 378, https://doi.org/10.3390/bioengineering9080378.
[106] C. Kryou, I. Theodorakos, P. Karakaidos, A. Klinakis, A. Hatziapostolou, I. Zergioti, Parametric study of jet/droplet formation process during LIFT printing of living cell-laden bioink, Micromachines 12 (2021) 1408, https://doi.org/10.3390/mi12111408.
[107] S.D. Dutta, K. Ganguly, M.-S. Jeong, D.K. Patel, T.V. Patil, S.-J. Cho, K.-T. Lim, Bioengineered lab-grown meat-like constructs through 3D bioprinting of antioxidative protein hydrolysates, ACS Appl. Mater. Interfaces 14 (2022) 34513–34526, https://doi.org/10.1021/acsami.2c10620.
[108] D. Trucco, A. Sharma, C. Manferdini, E. Gabusi, M. Petretta, G. Desando, L. Ricotti, J. Chakraborty, S. Ghosh, G. Lisignoli, Modeling and fabrication of silk fibroin–gelatin-based constructs using extrusion-based three-dimensional bioprinting, ACS Biomater. Sci. Eng. 7 (2021) 3306–3320, https://doi.org/10.1021/acsbiomaterials.1c00410.
[109] M. Di Giuseppe, N. Law, B. Webb, R.A. Macrae, L.J. Liew, T.B. Sercombe, R. J. Dilley, B.J. Doyle, Mechanical behaviour of alginate-gelatin hydrogels for 3D bioprinting, J. Mech. Behav. Biomed. Mater. 79 (2018) 150–157, https://doi.org/10.1016/j.jmbbm.2017.12.018.
[110] A. Shehzad, F. Mukasheva, M. Moazzam, D. Sultanova, B. Abdikhan, A. Trifonov, D. Akilbekova, Dual-crosslinking of gelatin-based hydrogels: promising compositions for a 3D printed organotypic bone model, Bioengineering 10 (2023) 704, https://doi.org/10.3390/bioengineering10060704.
[111] A.A. Aldana, F. Valente, R. Dilley, B. Doyle, Development of 3D bioprinted GelMA-alginate hydrogels with tunable mechanical properties, Bioprinting 21 (2021) e00105, https://doi.org/10.1016/j.bprint.2020.e00105.
[112] W. Li, M. Wang, L.S. Mille, J.A. Robledo Lara, V. Huerta, T. Uribe Velázquez, F. Cheng, H. Li, J. Gong, T. Ching, C.A. Murphy, A. Lesha, S. Hassan, T.B. F. Woodfield, K.S. Lim, Y.S. Zhang, A smartphone-enabled portable digital light processing 3D printer, Adv. Mater. 33 (2021), https://doi.org/10.1002/adma.202102153.
[113] J. Huh, Y.-W. Moon, J. Park, A. Atala, J.J. Yoo, S.J. Lee, Combinations of photoinitiator and UV absorber for cell-based digital light processing (DLP) bioprinting, Biofabrication 13 (2021) 034103, https://doi.org/10.1088/1758-5090/abfd7a.
[114] N. Anandakrishnan, H. Ye, Z. Guo, Z. Chen, K.I. Mentkowski, J.K. Lang, N. Rajabian, S.T. Andreadis, Z. Ma, J.A. Spernyak, J.F. Lovell, D. Wang, J. Xia, C. Zhou, R. Zhao, Fast stereolithography printing of large-scale biocompatible hydrogel models, Adv. Healthcare Mater. 10 (2021), https://doi.org/10.1002/adhm.202002103.
[115] Y. Yao, A. Molotnikov, H.C. Parkington, L. Meagher, J.S. Forsythe, Extrusion 3D bioprinting of functional self-supporting neural constructs using a photoclickable gelatin bioink, Biofabrication 14 (2022) 035014, https://doi.org/10.1088/1758-5090/ac6e87.
[116] S.D. Dutta, T.V. Patil, K. Ganguly, A. Randhawa, R. Acharya, M. Moniruzzaman, K.-T. Lim, Trackable and highly fluorescent nanocellulose-based printable bio-resins for image-guided tissue regeneration, Carbohydr. Polym. 320 (2023) 121232, https://doi.org/10.1016/j.carbpol.2023.121232.
[117] A. Mörö, S. Samanta, L. Honkamäki, V.K. Rangasami, P. Puistola, M. Kauppila, S. Narkilahti, S. Miettinen, O. Oommen, H. Skottman, Hyaluronic acid based next generation bioink for 3D bioprinting of human stem cell derived corneal stromal model with innervation, Biofabrication 15 (2023) 015020, https://doi.org/10.1088/1758-5090/acab34.
[118] T.B. Ngo, B.S. Spearman, N. Hlavac, C.E. Schmidt, Three-dimensional bioprinted hyaluronic acid hydrogel test beds for assessing neural cell responses to competitive growth stimuli, ACS Biomater. Sci. Eng. 6 (2020) 6819–6830, https://doi.org/10.1021/acsbiomaterials.0c00940.
[119] J.H. Galarraga, A.P. Dhand, B.P. Enzmann, J.A. Burdick, Synthesis, characterization, and digital light processing of a hydrolytically degradable hyaluronic acid hydrogel, Biomacromolecules 24 (2023) 413–425, https://doi.org/10.1021/acs.biomac.2c01218.
[120] R. Rizzo, N. Petelinšek, A. Bonato, M. Zenobi-Wong, From free-radical to radical-free: a paradigm shift in light-mediated biofabrication, Adv. Sci. 10 (2023), https://doi.org/10.1002/advs.202205302.
[121] P. Dorishetty, R. Balu, A. Gelmi, J.P. Mata, A. Quigley, N.K. Dutta, N. R. Choudhury, Microporosity engineered printable silk/graphene hydrogels and their cytocompatibility evaluations, Mater Today Adv 14 (2022) 100233, https://doi.org/10.1016/j.mtadv.2022.100233.
[122] W. Boonlai, N. Hirun, K. Suknuntha, V. Tantishaiyakul, Development and characterization of pluronic F127 and methylcellulose based hydrogels for 3D bioprinting, Polym. Bull. 80 (2023) 4555–4572, https://doi.org/10.1007/s00289-022-04271-6.
[123] S. Coşkun, S.O. Akbulut, B. Sarıkaya, S. Çakmak, M. Gümüşderelioğlu, Formulation of chitosan and chitosan-nanoHAp bioinks and investigation of printability with optimized bioprinting parameters, Int. J. Biol. Macromol. 222 (2022) 1453–1464, https://doi.org/10.1016/j.ijbiomac.2022.09.078.
[124] H. Xu, J. Casillas, S. Krishnamoorthy, C. Xu, Effects of Irgacure 2959 and lithium phenyl-2,4,6-trimethylbenzoylphosphinate on cell viability, physical properties, and microstructure in 3D bioprinting of vascular-like constructs, Biomed. Mater. 15 (2020) 055021, https://doi.org/10.1088/1748-605X/ab954e.
[125] S. Kumari, P. Mondal, K. Chatterjee, Digital light processing-based 3D bioprinting of κ-carrageenan hydrogels for engineering cell-loaded tissue scaffolds, Carbohydr. Polym. 290 (2022) 119508, https://doi.org/10.1016/j.carbpol.2022.119508.
[126] K.S. Lim, B.J. Klotz, G.C.J. Lindberg, F.P.W. Melchels, G.J. Hooper, J. Malda, D. Gawlitta, T.B.F. Woodfield, Visible light cross-linking of gelatin hydrogels offers an enhanced cell microenvironment with improved light penetration depth, Macromol. Biosci. 19 (2019), https://doi.org/10.1002/mabi.201900098.
[127] A.M. Navara, Y.S. Kim, Y. Xu, C.L. Crafton, M. Diba, J.L. Guo, A.G. Mikos, A dual-gelling poly(N-isopropylacrylamide)-based ink and thermoreversible poloxamer support bath for high-resolution bioprinting, Bioact. Mater. 14 (2022) 302–312, https://doi.org/10.1016/j.bioactmat.2021.11.016.
[128] S. England, A. Rajaram, D.J. Schreyer, X. Chen, Bioprinted fibrin-factor XIII-hyaluronate hydrogel scaffolds with encapsulated Schwann cells and their in vitro characterization for use in nerve regeneration, Bioprinting 5 (2017) 1–9, https://doi.org/10.1016/j.bprint.2016.12.001.
[129] B.B. Mendes, M. Gómez-Florit, A.G. Hamilton, M.S. Detamore, R.M. A. Domingues, R.L. Reis, M.E. Gomes, Human platelet lysate-based nanocomposite bioink for bioprinting hierarchical fibrillar structures, Biofabrication 12 (2019) 015012, https://doi.org/10.1088/1758-5090/ab33e8.
[130] A. Schwab, R. Levato, M. D'Este, S. Piluso, D. Eglin, J. Malda, Printability and shape fidelity of bioinks in 3D bioprinting, Chem. Rev. 120 (2020) 11028–11055, https://doi.org/10.1021/acs.chemrev.0c00084.
[131] A. Ribeiro, M.M. Blokzijl, R. Levato, C.W. Visser, M. Castilho, W.E. Hennink, T. Vermonden, J. Malda, Assessing bioink shape fidelity to aid material development in 3D bioprinting, Biofabrication 10 (2017) 014102, https://doi.org/10.1088/1758-5090/aa90e2.
[132] J. Guan, S. You, Y. Xiang, J. Schimelman, J. Alido, X. Ma, M. Tang, S. Chen, Compensating the cell-induced light scattering effect in light-based bioprinting using deep learning, Biofabrication 14 (2022) 015011, https://doi.org/10.1088/1758-5090/ac3b92.
[133] S. You, Y. Xiang, H.H. Hwang, D.B. Berry, W. Kiratitanaporn, J. Guan, E. Yao, M. Tang, Z. Zhong, X. Ma, D. Wangpraseurt, Y. Sun, T. Lu, S. Chen, High cell density and high-resolution 3D bioprinting for fabricating vascularized tissues, Sci. Adv. 9 (2023), https://doi.org/10.1126/sciadv.ade7923.
[134] X. Huang, W.L. Ng, W.Y. Yeong, Predicting the number of printed cells during inkjet-based bioprinting process based on droplet velocity profile using machine learning approaches, J. Intell. Manuf. 35 (2024) 2349–2364, https://doi.org/10.1007/s10845-023-02167-4.
[135] C.W. Beh, D.S. Yew, R.J. Chai, S.Y. Chin, Y. Seow, S.S. Hoon, A fluid-supported 3D hydrogel bioprinting method, Biomaterials 276 (2021) 121034, https://doi.org/10.1016/j.biomaterials.2021.121034.
[136] Y. Lee, J.A. Park, T. Tuladhar, S. Jung, Sonochemical degradation of gelatin methacryloyl to control viscoelasticity for inkjet bioprinting, Macromol. Biosci. 23 (2023), https://doi.org/10.1002/mabi.202200509.
[137] C. He, Y. Sun, N. Liu, K. Yu, Y. Qian, Y. He, Formation theory and printability of photocurable hydrogel for 3D bioprinting, Adv. Funct. Mater. 33 (2023), https://doi.org/10.1002/adfm.202301209.
[138] C. Afting, P. Mainik, C. Vazquez-Martel, T. Abele, V. Kaul, G. Kale, K. Göpfrich, S. Lemke, E. Blasco, J. Wittbrodt, Minimal-invasive 3D laser printing of microimplants in organismo, Adv. Sci. 11 (2024), https://doi.org/10.1002/advs.202401110.
[139] W.L. Ng, X. Huang, V. Shkolnikov, R. Suntornnond, W.Y. Yeong, Polyvinylpyrrolidone-based bioink: influence of bioink properties on printing performance and cell proliferation during inkjet-based bioprinting, Biodes Manuf 6 (2023) 676–690, https://doi.org/10.1007/s42242-023-00245-3.